TEMPORAL AND SPATIAL PATTERNS OF SEA-LEVEL RISE IMPACTS TO COASTAL WETLANDS AND OTHER ECOSYSTEMS

A THESIS SUBMITTED TO THE GRADUATE DIVISION OF THE
UNIVERSITY OF HAWAIʻI AT MĀNOA IN PARTIAL FULFILLMENT OF THE
REQUIREMENTS FOR THE DEGREE OF

MASTERS OF SCIENCE

IN

GEOLOGY AND GEOPHYSICS

MAY 2014

By

Haunani H. Kane

Dissertation Committee

Charles Fletcher, Chairperson
L. Neil Frazer
Scott Rowland

Keywords: sea level rise, critical elevation, LiDAR, digital elevation model, Hawaii, expert judgment, adaptive management, wetlands, Hawaii, vulnerability

Acknowledgements

I would first like to thank my advisor, Chip Fletcher for providing guidance and pushing me to be the best that I can be. I am also very grateful to Neil Frazer for his patience, and encouragement. Thank you Scott Rowland for helping me to refine my manuscript, and your thoughtful comments. The research described in this dissertation was carried out with the help of present and former members of the University of Hawai‘i Coastal Geology Group, including Matthew Barbee, Tiffany Anderson, Brad Romine, and Shelly Habel. Mahalo Martin Vermeer for providing sea-level rise data. This work was made possible through funding and support from the Pacific Islands Climate Change Cooperative; School of Ocean Earth Science and Technology; Native Hawaiian Science and Engineering Mentorship Program; Kamehameha Schools ‘Imi Na‘auao; and the J. Watumull Merit Scholarship. Finally I would like to thank my ‘ohana and my friends who continue to inspire me to better, stronger, and wiser. Mahalo piha.

Abstract

Increased water levels, erosion, salinity, and flooding associated with sea-level rise threaten coastal and wetland habitats of endangered waterbirds, sea turtles, monk seals, and migratory shorebirds. As sea-level rises the greatest challenge will be prioritizing management actions in response to impacts. We provide decision makers with two solutions to adaptively manage the impacts of sea-level rise and apply these methods to three coastal wetland environments at Keālia National Wildlife Refuge (south Maui), Kanaha State Wildlife Sanctuary (north Maui), and James Campbell National Wildlife Refuge (north O‘ahu). Firstly, due to the low gradient of most coastal plain environments, the rate of sea-level rise impact will rapidly accelerate once the height of the sea surface exceeds a critical elevation. We calculate a local sea-level rise critical elevation and joint uncertainty that marks the end of the slow phase of flooding and the onset of rapid flooding. This critical transition period provides an important planning target for achieving adaptive management. Secondly, within highly managed coastal areas, landscape vulnerability is related to the site-specific goals of coastal stakeholders. We develop a threat-ranking process that defines vulnerability from a management perspective by identifying those parameters that best characterize how sea-level rise will impact decision maker’s ability to accomplish mandated goals and objectives. We also provide maps of sea-level rise impacts for each wetland that characterize these two solutions as well as highlight the geographic distribution of potential vulnerabilities. The tools developed here can be used as a guide to initiate and implement adaptation strategies that meet the challenges of sea-level rise in advance of the largest impacts.

Table of contents

LIST OF TABLES

LIST OF FIGURES

Chapter 1

INTRODUCTION

Accelerated sea-level rise (SLR) due to climate change threatens coastal communities and natural resources worldwide. It is estimated that 20% of the world's wetlands may be lost to SLR by the year 2080 (Nicholls 2004). The major impacts of SLR to coastal wetlands include habitat change and loss due to increased pond water levels and salinity, coastal erosion (Romine et al. 2013), wave overtopping (Vitousek et al. 2009), and increased frequency and severity of extreme high water events (Tebaldi et al. 2012).

To date, the majority of insular SLR vulnerability research has focused on summarizing impacts at a global scale (e.g. Wetzel et al. 2012; Bellard et al. 2013). Few studies have examined the consequences of SLR on the local biodiversity of low-elevation island ecosystems (Reynolds et al. 2012). Working closely with coastal stakeholders in Hawai'i we developed tools to guide the prioritization of conservation actions and initiate decision to adaptively manage SLR impacts.

Spatial variability of SLR

Before we can begin developing strategies to adaptively manage SLR impacts, we must first understand the physical factors that drive SLR. SLR projections and current rates are often described in a global context, however in reality there are spatial variations of SLR superimposed on a global average rise (Sallenger et al. 2012). Local or relative sea-level depends upon a number of different factors including changes in terrestrial ice mass (e.g. melting of glaciers and ice sheets), changes ocean temperature, and glacial isostatic adjustment (GIA).

As glaciers and ice sheets melt, they directly add fresh water to the ocean increasing sea-level. Due to gravitational forces, land ice attracts ocean water and when it melts the gravitational attraction of the ice sheet weakens decreasing the relative sea-level near the ice in the polar regions and increasing sea-level in the far field near the tropics (Spada et al. 2013). Recent studies show that all alpine glacial regions as well as the Antarctic and Greenland ice sheets are losing mass (Figure 1.1; Figure 1.2) (Gardner et al. 2013; Rignot et al. 2011).

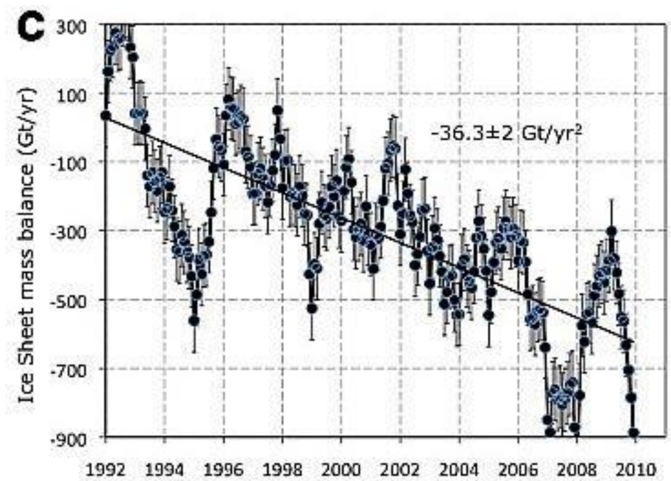

Figure 1.1. Total ice sheet mass balance (dm/dt) between 1992 and 2009 for Greenland and Antarctica (Rignot et al. 2011). The acceleration in ice sheet mass balance measured in gigatons per year squared is noted in the figure above.

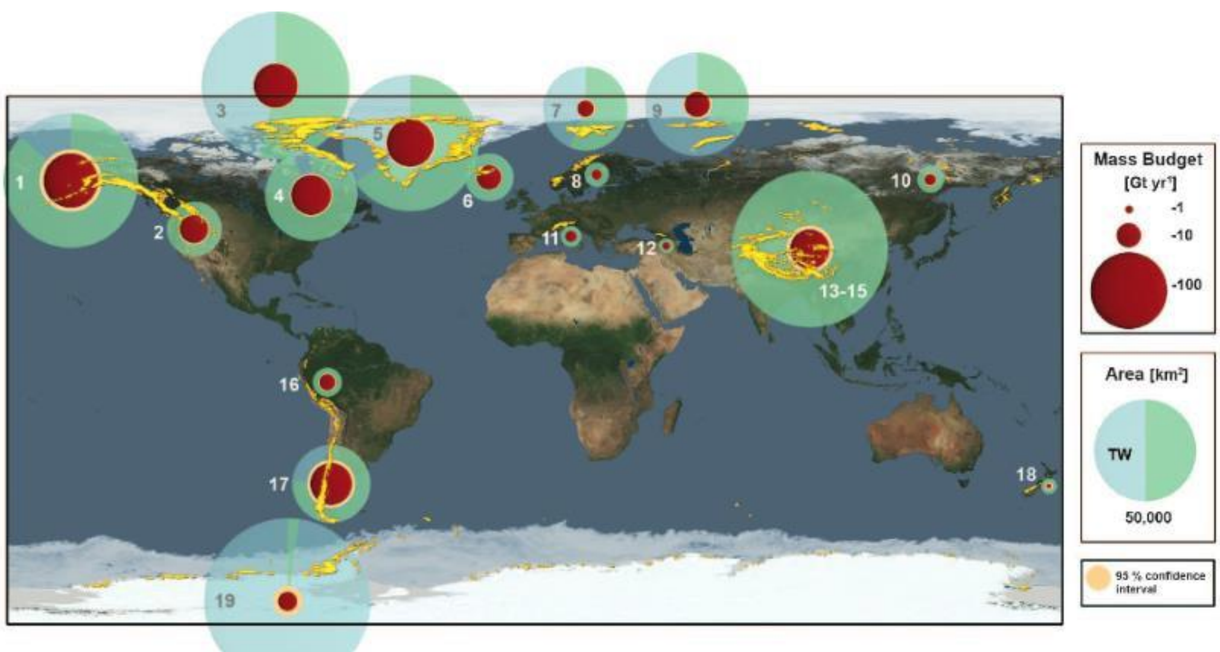

Figure 1.2. Regional glacier mass budgets and areas (Gardner et al. 2013). Red circles show 2003-2009 regional glacier mass budgets, and light blue/green circles show regional glacier areas with tidewater basin fractions (the extent of ice flowing into the ocean) in blue shading. The 95% CI in mass change estimates is represented by peach but is visible only in regions with large uncertainties.

Increases in atmospheric temperature warm seawater, increasing its volume and subsequent sea-level, a process known as thermal expansion. Climate models predict that even if greenhouse gas emissions cease rising and some excess CO_2 is removed from the atmosphere, SLR will persist for many centuries due to thermal expansion of deep ocean water (Meehl et al. 2012).

GIA is the response of the Earth's crust to changes in ice mass throughout the last glacial cycle. Approximately 20,000 years ago during the last glacial maximum large portions of the northern hemisphere were covered by continental glaciers, which caused a redistribution of Earth's internal mass and surface (Slangen et al. 2012). As the ice began to melt there was a delayed (viscoelastic) response of the lithosphere that continues to this day.

In addition to changes in ice mass, ocean responses, and GIA, local subsidence also plays a role in sea-level variability among the Hawaiian Islands. Along the Hawaiian archipelago variability in long term SLR rates may be related to variations in lithospheric flexure with distance from the actively growing Hawaiʻi Island (Moore 1987) and/or decadal variations in upper ocean water masses (Caccamise et al. 2005). A general trend of decreasing SLR rates is observed to the northwest from the younger islands of Hawaiʻi and Maui (Hawaiʻi: 3.27 ± 0.7 mm/yr, and 2.32 ± 0.53 mm/yr resp.) towards Oʻahu (Oʻahu: 1.50 ± 0.25 mm/yr) (http://tidesandcurrents.noaa.gov) (Figure 1.3). Hawaiʻi Island experiences a SLR rate comparable to the global average (3.2 ± 0.4 mm/yr) recorded by satellite data from 1993 to 2009 (Church and White 2011).

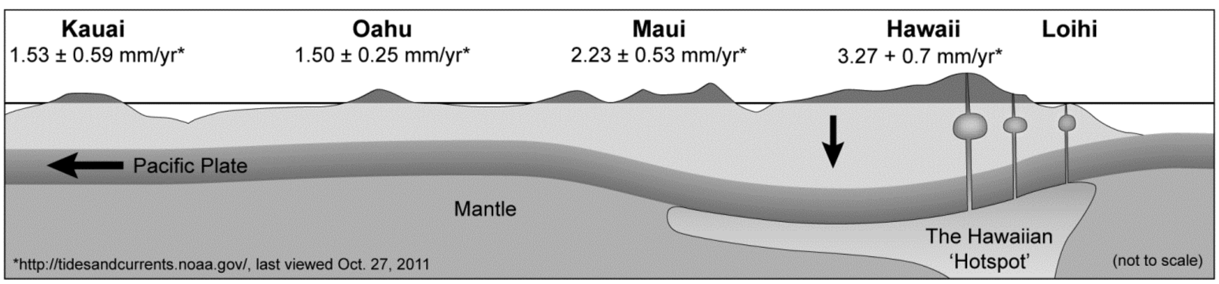

Figure 1.3. Mean sea-level trends recorded at Hawaiʻi tide stations (modified after Romine et al. 2013).

Current SLR models

The spatial variability of end of the century sea-level has been modeled by two regional SLR models. A coupled global circulation model predicts that under scenarios of rapid melting Central Pacific sea-level by the end of the century will be 1.12-1.17 m above present (Slangen et al. 2012) (Figure 1.4). A second regional model by Spada et al. (2013), improves upon terrestrial ice mass estimates and concludes that terrestrial ice mass is the main source of SLR rather than the ocean response as modeled by Slangen et al. (2012). Considering terrestrial ice mass and ocean response contributions to SLR, a mid-range model predicts an end of century sea-level increase of 0.5-0.75 m and the high end model predicts an increase of 1.0-1.5 m for the Central Pacific (Spada et al. 2013). The value of regional SLR models is that they allow us to infer the Hawaiian Islands departure from the global average. Yet it has been argued that regional SLR models are not yet ready for direct use because they fail to capture observed local weather patterns, local subsidence, produce inconsistencies among projections, and are not associated with a SLR curve from which we can produce yearly SLR values (Tebaldi et al. 2012).

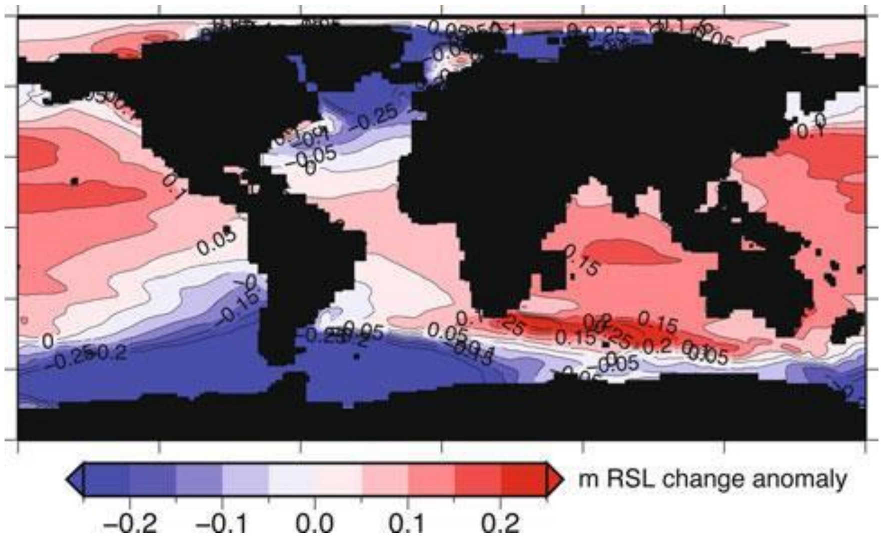

Figure 1.4. Mean seasonal sea-level anomaly (m) with respect to a global mean regional sea-level change of 1.02 m for the year 2100 (Slangen et al. 2011). Sea-level in Hawai‘i is predicted to be 0.1-0.15 m above the global average, corresponding to a 1.12-1.17 rise in total sea-level.

Regional models provide insight into the spatial variability of SLR, however we apply global SLR rates to Hawai‘i because regional models fail to capture observed local weather patterns, local subsidence, produce inconsistencies among projections (Tebaldi et al. 2012), and map SLR for only one point in time.

A number of global SLR estimates have been created for the year 2100 and beyond using physical modeling (e.g.: Slangen et al. 2012, Spada et al. 2013), semi-empirical methods (eg: Vermeer and Rahmstorf 2009; Jerejeva et al. 2012), and expert judgment assessment (NRC 2012; Bamber and Aspinall 2013; Horton et al. 2014) (Table 1.1). Semi-empirical and expert judgment methods serve as alternatives to models based on physical processes because dynamic systems such as ice sheets are not yet fully understood (IPCC, 2007; Vermeer et al. 2012). In particular the semi-empirical method of Vermeer and Rahmstorf (2009) offers a unique solution for the position of future sea-levels by providing yearly global values for multiple economic emission scenarios. Vermeer and Rahmstorf (2009) compute mean sea-level curves and associated uncertainty (1σ) bands across the 19 climate models used in the Intergovernmental Panel on Climate Change (IPCC) fourth assessment report (AR4) (2007) . The robustness of Vermeer and Rahmstorf's (2009) projections of future SLR are documented by Rahmstorf et al. (2011).

Table 1.1 Global sea-level (m) estimates for the year 2100 based upon expert judgment assessment, semi-empirical methods, and physical modeling methods.

Expert judgment assessment			Semi-empirical		Physical (Ocean coupled model)		
National Research Council (NRC 2012)	Bamber and Aspinall (2013)	Horton et al. (2014)	Vermeer & Ramstorf (2009)	Jerejeva (2010)	*Slangen et al. (2012)	*Spada et al. (2013)	IPCC AR5 (Church et al. 2013)
0.5 - 1.4	0.33 – 1.32	0.6 – 1.2	0.75 - 1.9	0.6-1.9	1.12 – 1.17	0.5 –1.5	0.26 -0.98

*Central Pacific sea-level estimate. All other SLR projections are global estimates.

The IPCC's fifth assessment report (AR5) released in September 2013 builds upon AR4 and incorporates new evidence of climate change, including SLR data (IPCC 2013). Improved understanding of the physical components of SLR, better agreement among process-based models with observations, and improved modeling of land-ice contributions has resulted in more robust SLR predictions. A new set of scenarios, the Representative Concentration Pathways (RCPs) was used to model climate for the end of the 21st century (2081-2100) relative to 1986-2006. AR5 predicts that global mean SLR for 2081-2100 will likely be in the range of 0.26-0.55 m for the best case scenario (RCP2.6) and 0.45 to 0.82 m for the worst case scenario (RCP8.5). By the end of the century RCP8.5 projects a 0.98 rise in global mean sea-level.

In this study we provide decision makers with two solutions to adaptively manage the impacts of SLR and apply these methods to three coastal wetland environments at Keālia National Wildlife Refuge (south Maui), Kanaha State Wildlife Sanctuary (north Maui), and James Campbell National Wildlife Refuge (north O‘ahu). Chapter two of this dissertation presents a method by which we calculate a local SLR critical elevation and joint uncertainty that marks the end of the slow phase of flooding and the onset of rapid flooding. This critical transition period provides an important planning target for achieving adaptive management. Secondly, in chapter 3 we develop a threat-ranking process that defines vulnerability from a management perspective by identifying those parameters that best characterize how SLR will impact decision maker's ability to accomplish mandated goals and objectives.

The methodologies used here are flexible and may be applied to new SLR models as global and regional projections improve. Based upon the quality of projections available relative to the timing of this project we apply Vermeer and Rahmstorf's (2009) projections to the methods of chapter 2, and the IPCC AR5 projections to chapter 3.

CHAPTER 2

DECISION-MAKERS FACE A "CRITICAL ELEVATION" OF FLOODING DUE TO SEA-LEVEL RISE

Haunani H. Kane, Charles H. Fletcher, Neil L. Frazer, and Matthew M. Barbee

Abstract

Coastal strand and wetland habitats are intensively managed to restore and maintain populations of endangered species. However, sea-level rise (SLR) threatens the work of wetland and coastal managers because coastal erosion, salt-water intrusion, and flooding degrade critical habitats. Because habitat loss is a measure of the risk of extinction, managers are keen to receive guidelines and other tools to reduce the risk posed by SLR. Due to the low gradient of most coastal plain environments, the rate of SLR impact will rapidly accelerate once the height of the sea surface exceeds a critical elevation. Here we develop this concept by calculating a SLR critical elevation and joint uncertainty that distinguishes between slow and rapid phases of flooding at three coastal wetlands on the Hawaiian islands of Maui and Oʻahu. Using high resolution LiDAR digital elevation models (DEMs) we map and rank areas flooded from high (80%) to low (2.5%) risk based upon the percent probability of flooding under the B1, A2, and A1Fl economic emissions scenarios. Across the critical elevation, the area of wetland (expressed as a percentage of the total) at high risk of flooding under the A1Fl scenario increased from 21.0% to 53.3% (south Maui), 0.3% to 18.2% (north Maui), and 1.7% to 15.9% (north Oʻahu). At the same time, low risk areas increased from 34.1% to 80.2%, 17.7% to 46.9%, and 15.4% to 46.3%, resp. These results indicate that the critical elevation of SLR may have already passed (2003) on south Maui, and that decision makers may have approximately 37 years (2050) on North Maui and Oʻahu to conceive, develop, and implement adaptation strategies that meet the challenges of SLR in advance of the largest impacts.

Introduction

Few studies have examined the consequences of SLR on the biodiversity of low-elevation island ecosystems (Reynolds et al. 2012). Hawaiʻi, the most isolated island group, is a hotspot for unique organisms, and comprises the greatest number of endangered species of any state in the United States (U.S.) (Dobson et al. 1997). Increased water levels, erosion, salinity, and flooding associated with SLR threatens the habitats of endangered waterbirds, sea turtles, Hawaiian monk seals, and migratory shorebirds. In addition, many coastal wetlands are used for subsistence fish farming as well as taro (*Colocasia esculenta)* agriculture, which, in cultural practice, is believed to be the original ancestor of the Hawaiian people.

In comparison to the continental U.S., the management of Pacific Island wetlands is fairly new. In 2011 a series of Comprehensive Conservation Plans were published for each of the Hawaiian Islands' national wildlife refuges (U.S. Fish and Wildlife Service 2011a, 2011b). These documents serve as the first attempt by local wetland managers to plan for the potential impacts of climate change.

Planning for the risks of SLR is challenging because impacts aren't immediately observable (Gesch 2009) on the timescales that wetlands are typically managed. The majority of regional and global SLR predictions are projected for the year 2100 (e.g. Slangen et al. 2012; Spada et al. 2013; Vermeer and Rahmstorf 2009) and beyond (e.g. Jevrejeva et al. 2012; Meehl et al. 2012; Schaeffer et al. 2012), which exceeds the standard 15-year planning horizon of the Hawaiʻi wetland refuge system. Predicting SLR impacts on timescales of less than a century is largely limited by the uncertainty associated with global SLR projections (Church and White 2011) and the vertical uncertainty of topographic data used to create SLR vulnerability maps (Cooper et al. 2013b).

The objective of this study is to develop a methodology that identifies the onset of greatest impacts related to SLR. Our results provide a physical process-based planning horizon useful by decision-makers who are developing management strategies to meet the challenges of climate change. Our methodology supplements the typical 15-year planning timeframe with an estimate of when the greatest impacts related to SLR will occur. This approach will allow future generations to form flexible adaptation management plans based on prioritized (and changing) habitat needs as sea level rises.

For most coastal plain environments the rate of impact due to SLR flooding will rapidly accelerate once the height of the sea surface exceeds a critical elevation. Using a hypsometric model (Zhang 2011; Zhang et al. 2011) we identify the critical elevation marking the end of slow flooding and the onset of rapid flooding. Mapping each phase of flooding and establishing the chronology of impacts provides wetland decision-makers with valuable information about the height of sea-level that will produce the onset of the greatest innundation and the timeframe for which the bulk of wetland assets may be threatened.

Mapping SLR vulnerability

One way of communicating the risk of SLR is to map low lying areas using high resolution light detection and ranging (LiDAR) digital elevation models (DEMs). SLR inundation maps are created by "flooding" those raster DEM cells that have an elevation at or below a given modeled sea surface height (Gesch 2009).

Previous studies have considered only marine sources of inundation by mapping DEM cells that are hydrologically connected to the ocean through a continuous path of adjacent flooded cells (Gesch 2009; Poulter and Haplin 2008). Here, we consider both marine and groundwater inundation (Cooper et al. 2013a) because marine inundation alone underestimates SLR impacts (Rotzoll and Fletcher 2012) and does not account for rising groundwater tables (Bjerklie et al. 2012).

This is a reasonable assumption as water table elevations in coastal settings sit typically above mean sea-level (MSL) and are highly correlated with daily tides and other sources of marine energy (Rotzoll et al. 2008, Rotzoll and Fletcher 2012). In addition many of Hawaiʻi's wetlands are located just inland of a narrow coastal strand and are dependent upon natural or pumped groundwater sources to maintain pond water levels (Hunt and De Carlo 2000; U.S. Fish and Wildlife Service 2011a, 2011b).

For the purpose of this study we apply Vermeer and Rahmstorfs (2009) global SLR scenarios to assess the impacts of SLR flooding upon Hawaiian coastal ecosystems. The SLR curves provided by this model enable decision makers to correlate impacts of slow and rapid phases of flooding with a sea-level height and time. We encourage managers to plan for three scenarios of future sea-level. The B1 (1.04 m by 1200), A2 (1.24 m), and A1FI (1.43 m) scenarios encompass the range of SLR projections forecast by regional models (e.g., Spada et al. 2013) for Hawaiʻi by the end of the century. The methodology used here may be applied to new SLR models as global and regional projections improve.

Methods

We study three coastal wetlands in Hawaiʻi: 1) James Campbell National Wildlife Refuge (north Oʻahu), 2) Kanaha Pond State Wildlife Sanctuary (north Maui), and 3) Keālia Pond National Wildlife Refuge (south Maui; Figure 2.1). All three wetlands are intensively managed throughout the year to restore and maintain self-sustaining populations of endangered waterbirds including the Hawaiian Coot (*Fulica alai*), Hawaiian Moorhen (*Gallinula chloropus sandvicensis*), Hawaiian Stilt (*Himantopus mexicanus knudseni*), and the Hawaiian duck (*Anas wyvilliana*; U.S. Fish and Wildlife Service 2011c).

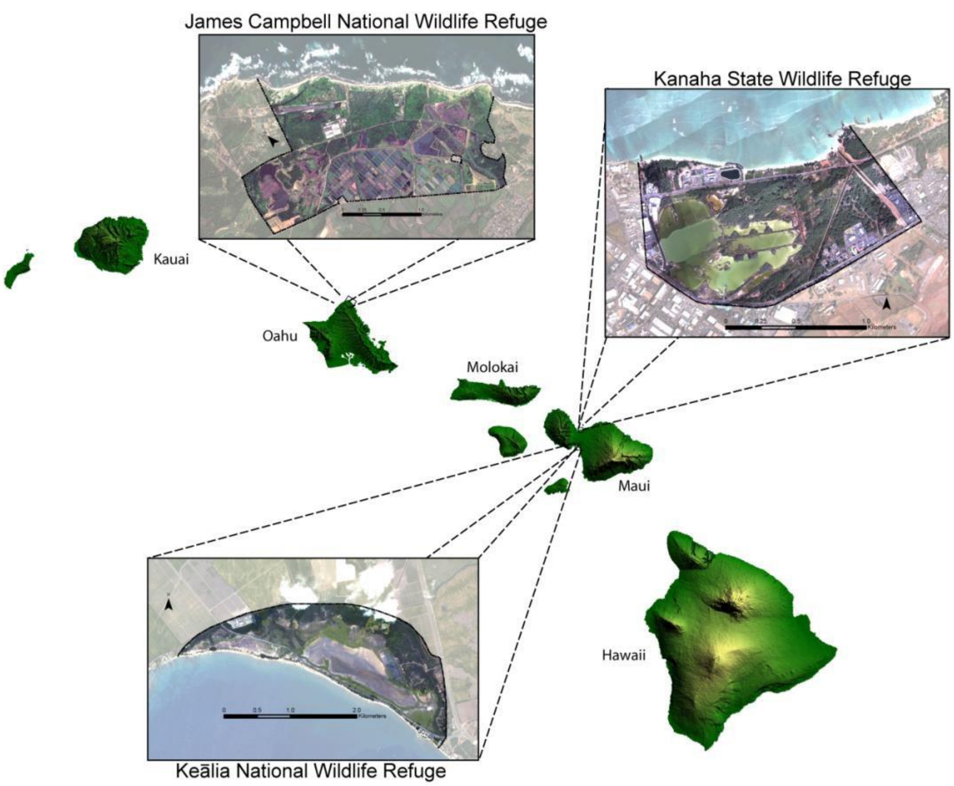

Figure 2.1. SLR impacts were assessed for James Campbell National Wildlife Refuge (north Oʻahu), Kanaha Pond State Wildlife Sanctuary (north Maui), and Keālia Pond National Wildlife Refuge (south Maui).

Springs, rainfall, and runoff feed these wetlands, however during the dry season managers may supplement pond water levels with additional sources of groundwater. Unlike temperate salt marshes, Hawai‘i’s coastal wetlands are microtidal, largely isolated from the ocean, and sediment sources include eolian dust, intermittent stream flooding during the wet season (October-April), and internally produced organic solids (U.S. Fish and Wildlife Service 2011a).

With the exception of narrow ocean outlet ditches at all three, the study sites are buffered from marine impacts by 2-4 m sand dunes and a narrow coastal strand. Depending upon the coastal strand for critical habitat are native plants, the endangered Hawaiian monk seal (*Monachus schauinslandi*), the threatened Hawaiian green sea turtle (*Chelonia mydas*), and migratory seabirds during winter months.

Data processing

The U.S. Army Corps of Engineers (USACE) collected airborne LiDAR data for James Campbell and Kanaha during January and February 2007. USACE metadata reports an average point spacing of 1.3 m and a vertical accuracy of better than $\pm$ 0.20 m (1σ). Airborne 1 collected LiDAR for Keālia in 2006 for the Federal Emergency Management Agency (FEMA) and reports average point spacing close to 0.30 m and an $RMSE_z$ of 0.18 m (Dewberry 2008). For the purpose of this study we assume the $RMSE_z$ and 1 are equivalent (NOAA 2010). LiDAR data were collected in geographic coordinates and ellipsoid heights relative to the North American Datum of 1983 (NAD83) and converted to orthometric heights using the Geiod03 model. These heights were adjusted to MSL based upon a 2006 epoch for the USACE dataset and a 2002 epoch for the FEMA dataset. Last return features, or bare earth LiDAR were converted from LAS format to ESRI shapefile format and reprojected to Universal Transverse Mercator (UTM) zone 4 North.

Triangular irregular networks (TINs) were derived from the processed and filtered LiDAR point data for each study area. To identify areas where point density poorly characterizes coastal morphology, a distance of 20 m (maximum edge length) was used to constrain the TIN extents. A 2 m horizontal resolution DEM was interpolated from each TIN using the nearest neighbor method to represent the corresponding bare earth topography.

Critical elevation

We use a land area hypsometric curve (Zhang 2011; Zhang et al. 2011) to identify a critical elevation and characterize the rate of flooding based upon local topography (Figure 2.2). We adhere closely to NOAA Coastal Services Center Coastal Inundation Toolkit Mapping Methodology (accessed at http://www.csc.noaa.gov/slr/viewer/assets/pdfs/Inundation_ Methods. pdf) and use DEMs to model the area flooded as sea-level is increased from 0-5.0 m.

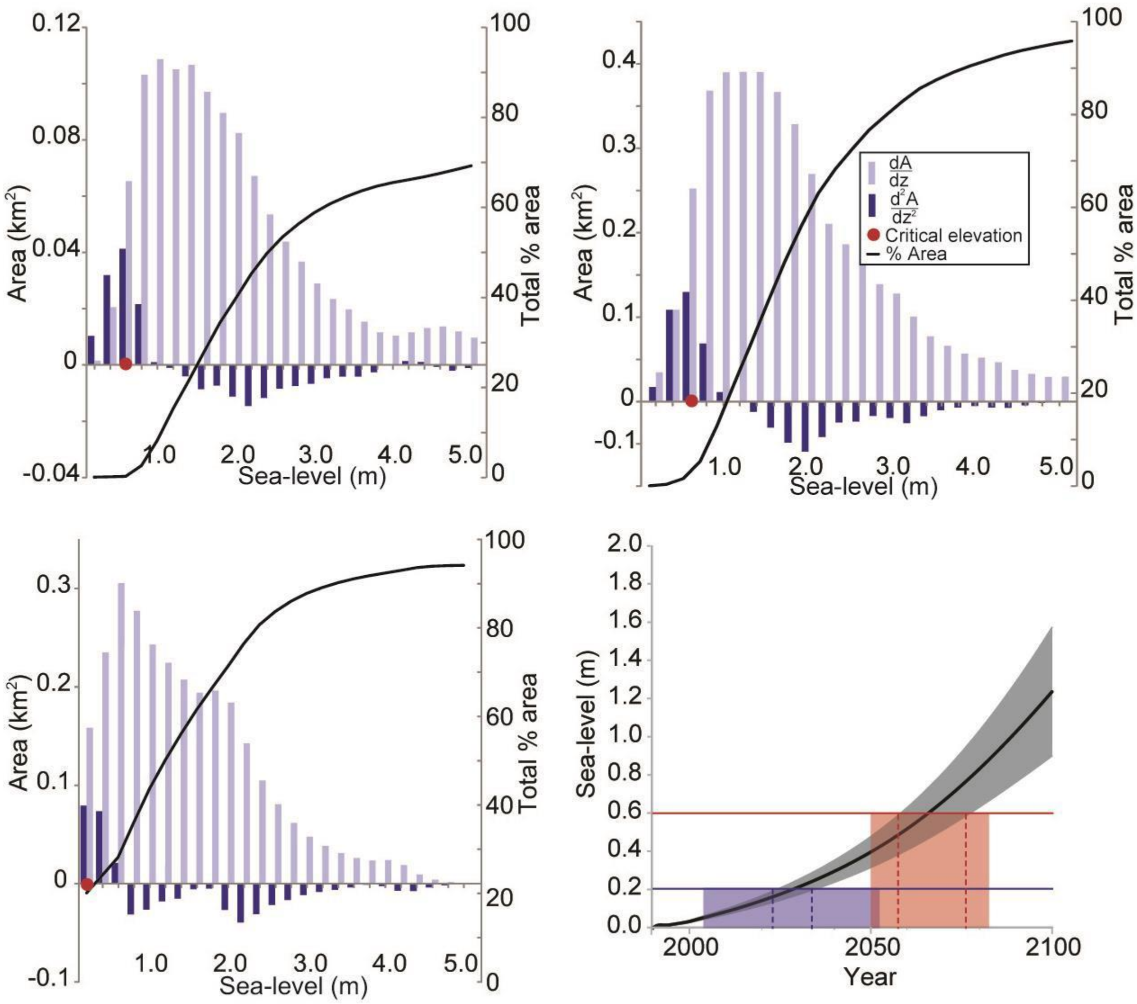

Figure 2.2 Land area hypsometric curves at Kanaha (a), James Campbell (b), and Keālia (c). The x-axis represents elevation (m) above MHHW. The y-axes represent total percent area at or below a corresponding sea-level value, and area (km^2) inundated as sea-level rises in 0.2 m increments. Temporal uncertainty of the critical elevation (d) is based upon the uncertainty of SLR projections alone (dashed lines) and the joint uncertainty of SLR projections and topography (shaded region).

Following the methodology of Cooper et al. (2013a) and due to the lack of a North American Vertical Datum of 1988 (NAVD 88) for Hawaiʻi, we map MSL values upon the 19-year epoch value of mean higher high water (MHHW) at the Honolulu tide gauge for James Campbell and at the Kahului tide gauge for Kanaha and Keālia to assess flooding at high tide (accessed at tidesandcurrents.noaa.gov). The hypsometric curve depicts the additional area that is flooded (dA) as sea-level is increased in increments of 0.20 m (this interval was chosen because it approximates the LiDAR vertical uncertainty). Combined with the SLR projection it gives the speed (dA/dt) and acceleration of flooding (d^2A/dz^2).

The critical elevation is identified at the sea-level at which d^2A/dz^2 is a maximum. For a linear rise in sea-level with time, the critical elevation separates flooding into a slow phase (relatively low dA/dt) and a fast phase (relatively high dA/dt). To determine the temporal uncertainty of each flooding phase we create a mixture distribution SLR curve from Vermeer and Rahmstorf's (2009) B1, A2, and A1FI SLR curves. The B1 (1.04 m by 2100), A2 (1.24 m), and A1FI (1.43 m) economic emission scenarios address how future global sea-level may change under different social, economic, technological, and environmental developments (IPCCC 2007). Assuming each scenario SLR curve is evenly weighted and normally distributed we calculate the total mean (and variance ( ) of the final SLR curve respectively:

$$\mu(t)=\frac{1}{3}\mu_{B1}(t)+\frac{1}{3}\mu_{A2}(t)+\frac{1}{3}\mu_{A1FI}(t) \tag{2.1}$$

$$\sigma^2(t)=\frac{1}{3}[(\mu_{B1}-\mu(t))^2+\sigma^2_{B1}]+\frac{1}{3}[(\mu_{A2}-\mu(t))^2+\sigma^2_{A2}]+\frac{1}{3}[(\mu_{A1FI}-\mu(t))^2+\sigma^2_{A1FI}] \tag{2.2}$$

From the SLR curve we calculate the temporal uncertainty of the critical elevation based upon SLR projections alone ( ) and SLR projections and topography (. This analysis allows us to determine whether incorporating hypsometry into management and planning makes a quantifiable difference.

$$\sigma_{t_s}=\frac{\sigma_s(t_T)}{\frac{d\mu_s(t_T)}{dt}} \tag{2.3}$$

$$\sigma_{t_{s+z}}=\frac{\sqrt{\sigma_s(t_T)^2+\sigma_Z(t_T)^2}}{\frac{d\mu_s(t_T)}{dt}} \tag{2.4}$$

Mapping the risk of flooding

We account for the uncertainty of SLR projections and LiDAR data in our SLR flood maps using a combination of several existing standards. Areas of high (80-100% probability), moderate (50-100% probability), and low (2.5-100% probability) risk are mapped using cumulative percent probability. The 80% probability contour identifies high confidence flood areas (NOAA 2010), whereas the 50% rank maps the area flooded by the predicted sea-level value alone. Gesch (2009) and the National Standard for

Spatial Data Accuracy (FGDC 1998) recommend the use of the linear error at the 95% confidence level (1.96 x $RMSE_z$) to identify additional areas that may be inundated at time *t*. The 2.5% rank used in this study to identify low risk areas equates to a standard-score of 1.96 when a cumulative or single tail approach is used (NOAA 2010).

To assess the percent probability that a location (x,y) will be inundated at time *t* we adhere closely to NOAA (2010) and Mitsova et al. (2012). For each economic scenario a 2 m horizontal resolution raster is created to calculate the expected height above MHHW (   ) at time *t*. We take the difference between the projected sea-level value above MHHW (   ) and the DEM elevation (   ):

$$\mu_h = \mu_s - \mu_z \tag{2.5}$$

To account for the uncertainty (   ) associated with an area's expected height above MHHW we combine two random and uncorrelated sources using summing in quadrature (Fletcher et al. 2003): SLR model uncertainty (   ) and LiDAR vertical uncertainty (   ).

$$\sigma_t = \sqrt{\sigma_s^2 + \sigma_z^2} \tag{2.6}$$

The SLR model uncertainty reflects a semi-empirical characterization of the physical link between climate change and SLR, and the LiDAR uncertainty is a measure of the vertical accuracy of the LiDAR points to represent the corresponding bare earth topography. A second surface is created to represent the standard-score (SS_{XY}) or the number of standard deviations a value falls from the mean.

$$SS_{XY} = \frac{\mu_h}{\sigma_t} \tag{2.7}$$

The standard-score raster is reclassified to a percent probability raster by means of a look-up table assuming normally distributed errors. Under each phase of SLR, we map and calculate the percent area with low, moderate, and high risk of flooding for the B1, A2, and A1FI scenarios. Re-engineered areas such as the diked ponds at James Campbell are not included in this analysis.

Results and Discussion

Defining a critical elevation

We identify a critical elevation that separates flooding into a slow and fast phase based upon the local topography of three coastal wetlands. The critical elevation of Keālia is defined at 0.2 m and is predicted to be exceeded by the year 2028 ± 25 years (Figure 2.2). Kanaha and James Campbell study areas are located at a slightly higher elevation resulting in a critical elevation of 0.6 m which will be reached by 2066 ± 16 years.

We acknowledge that the timeframe of exceedance for the critical elevation is quite large and is mostly a reflection of the quality of currently available data. To determine the critical elevation we deal with two sources of uncertainty; the uncertainty of the SLR model used to correlate sea-level with time, and the uncertainty of the LiDAR data used to identify and map the critical elevation. The large LiDAR uncertainty proves to be a major limiting factor. In comparison to considering SLR model uncertainty alone, accounting for the joint uncertainty of both datasets increases the temporal component of the critical elevation from ± 5 years to ± 25 years at Keālia and ± 9 years to ± 16 years at James Campbell and Kanaha. As SLR projections and topographic datasets improve, the methods used in this study can be employed with greater confidence.

Mapping SLR impacts for slow and fast phases of flooding

Here we find the slow phase of flooding is defined from present to 2028 ± 25 years (critical elevation = 0.2 m) at Keālia, and from present to 2066 ± 16 years (0.6 m) at Kanaha and James Campbell (Figure 2.3, 2.4, 2.5). To assist decision makers in prioritizing SLR impacts we map flooded areas of high, moderate, and low risk. Due to the similarity of SLR curves during the slow phase, all three economic scenarios agree that there is a moderate risk of 24.1% of Keālia, 2.8% of Kanaha, and 4.3% of James Campbell being flooded (Table 2.1). High and low risk areas encompass 21.0-34.1% of Keālia respectively, 0.3- 17.7% of Kanaha, and 1.7-15.4% of James Campbell. The slow phase of flooding represents the onset of vulnerability as SLR increases coastal erosion, and the extent and frequency of storm surges. Although initial percent area impacts may appear small, threatened areas include the majority of the coastline, and inland wetland environments at James Campbell and Keālia (Figure 2.3.).

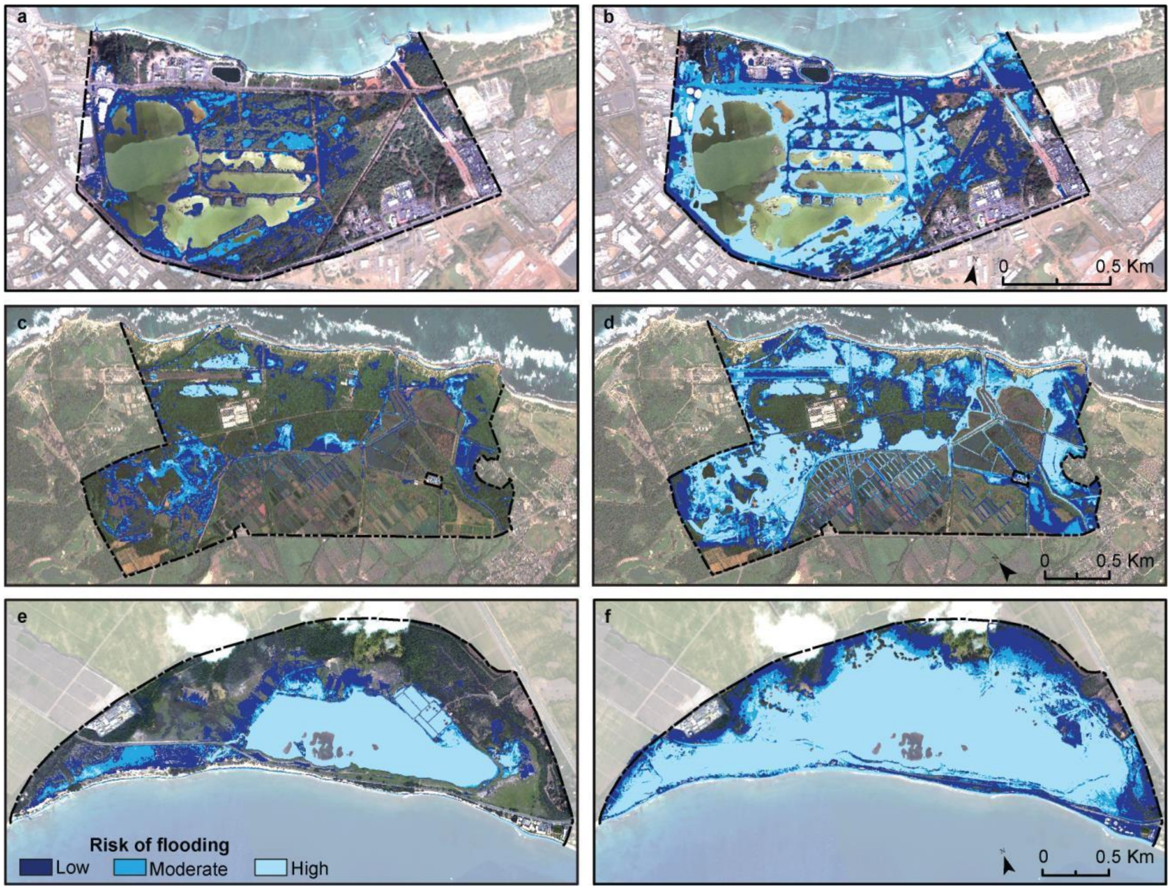

Figure 2.3. A1FI SLR risk comparison for slow (left column images) and fast phases of flooding at Kanaha (a-b) James Campbell (c-d), and Keālia (d-e).

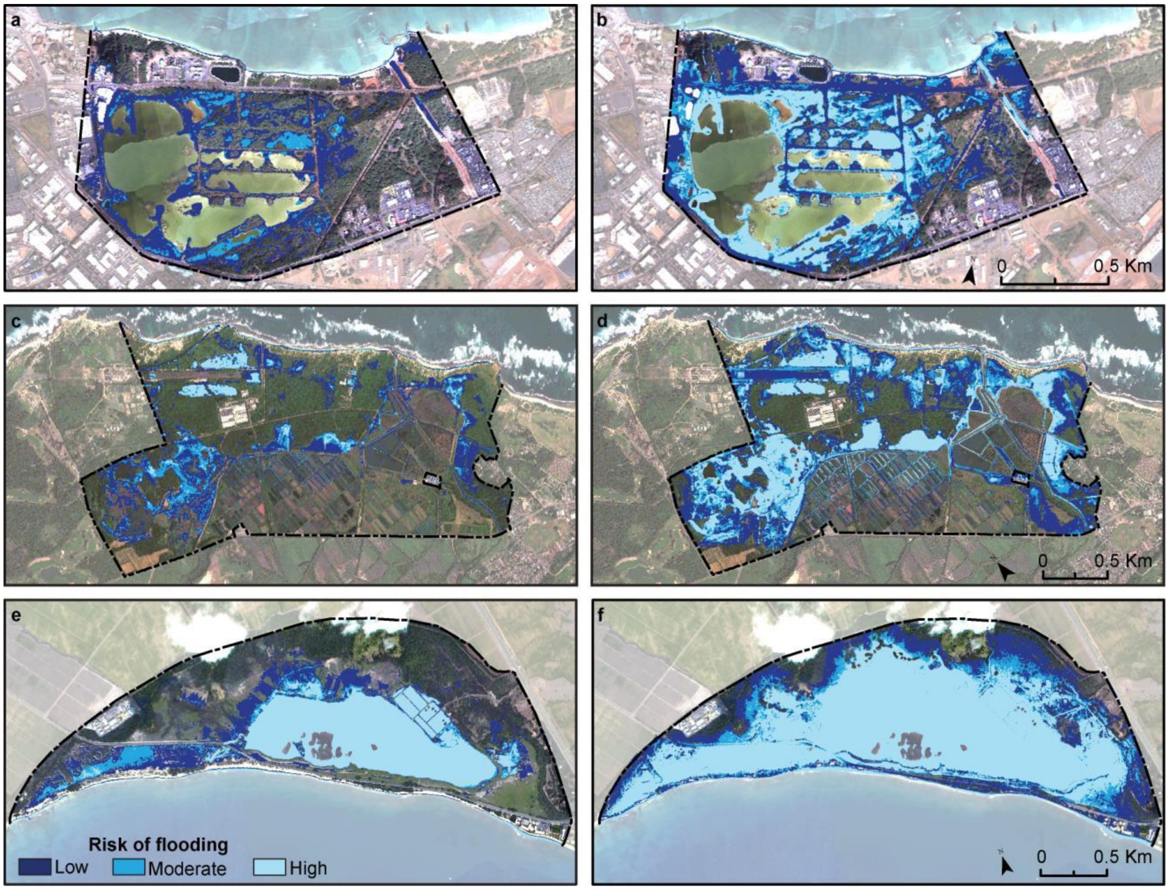

Figure 2.4. A2 SLR risk comparison for slow (left column images) and fast phases of flooding at Kanaha (a-b) James Campbell (c-d), and Keālia (d-e).

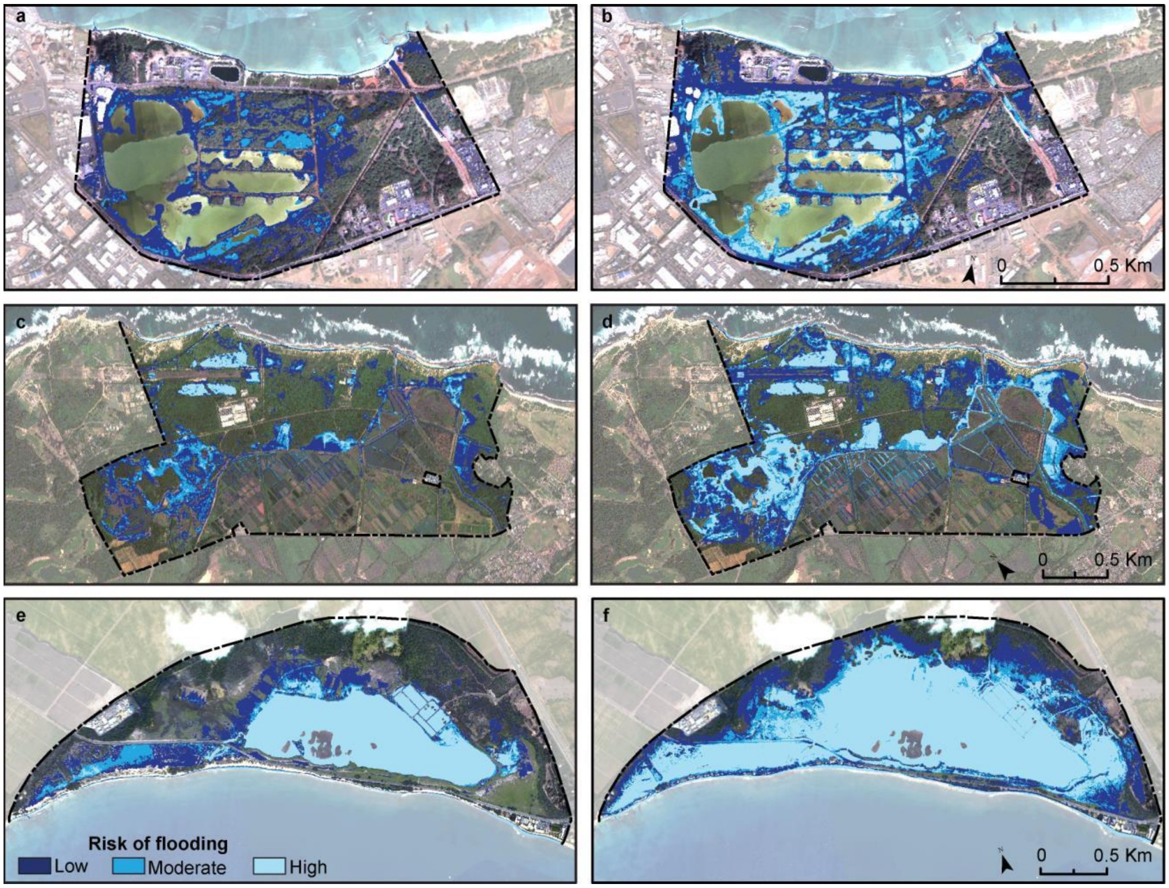

Figure 2.5. B1 SLR risk comparison for slow (left column images) and fast phases of flooding at Kanaha (a-b) James Campbell (c-d), and Keālia (d-e).

Table 2.1. Percent area of land vulnerable to high, low, and moderate risk for the slow and fast phase of flooding.

Study Area	Flooding Phase	Scenario	% Area High risk	% Area Moderate risk	% Area Low risk
James Campbell	Slow	B1, A2, A1FI	1.7	4.3	15.4
	Fast	B1	7.6	14.3	33.5
		A2	14.3	19.9	40.5
		A1FI	15.9	25.9	46.3
Kanaha	Slow	B1, A2, A1FI	0.3	2.8	17.7
	Fast	B1	7.0	16.4	36.2
		A2	13.2	22.6	43.2
		A1FI	18.2	28.8	49.6
Keālia	Slow	B1, A2, A1FI	21.0	24.1	34.1
	Fast	B1	42.7	51.3	67.6
		A2	48.5	57.0	74.1
		A1FI	53.3	62.2	80.2

The fast phase of flooding represents a time in which the bulk of impacts due to SLR are predicted to occur. We predict the fast phase of flooding will start in 2028 $\pm$ 25 years at Keālia and 2066 $\pm$ 16 years at Kanaha and James Campbell. These results indicate that the critical elevation of SLR may have already passed (2003) on south Maui, and that decision makers may have approximately 37 years (2050) on North Maui and O‘ahu to conceive, develop, and implement adaptation strategies that meet the challenges of SLR in advance of the largest impacts.

We do not model beyond 2100 because our SLR model does not exceed the year 2100. At 1.04 m (B1 projection for the year 2100) of SLR there is moderate risk of flooding for 51.3 % of Keālia, 16.4% of Kanaha, and 14.3% of James Campbell. At 1.24 m (A2), moderate risk SLR impacts increase to 57% of Keālia, 22.6% of Kanaha, and 19.9% of James Campbell. Under the worst case scenario of 1.43 (A1FI), moderate risk of flooding impacts increase to 62.2 % of Keālia, 28.8% of Kanaha, and 25.9% of James Campbell. SLR impacts experienced along the beaches during the slow phase expand and encroach into the upland vegetation and inland wetlands during the fast phase of flooding. At all 3 study areas, nearly all of the wetlands are subjected to moderate or low risk of flooding.

Strategies to manage SLR impacts

Hawai‘i, an area that represents less than 1% of the total U.S. land mass is home to approximately 27% of all federally listed threatened or endangered species in the U.S. (U.S. Fish and Wildlife Service 2011c; http://ecos.fws.gov/tess_public/pub/stateListingAndOccurrenceIndividual.jsp?state=HI&submit=G). Impacts associated with SLR exacerbate habitat loss, which is widely used as a measurement of the risk of extinction (Iwamura et al. 2013). Globally, resource managers will be challenged to preserve existing habitats through engineering, relocating habitats to higher elevations, and abandoning existing habitats when the magnitude of SLR overwhelms all other efforts.

Using the inundation maps provided in this study, wetland managers can begin prioritizing responses for the slow and rapid phases of SLR. Providing a critical elevation and a timeframe for the largest impacts of SLR enables wetland managers to begin formulating long-term adaptive management strategies beyond the typical 15 year time period. The methods used here are applied to wetlands in Hawai‘i, however they are applicable to all coastal stakeholders interested in managing resources and defining new policies in response to SLR.

Management efforts for the slow phase of flooding should be focused primarily on areas susceptible to moderate and high risk of flooding, specifically at the beaches and coastal strand. SLR will likely worsen the long term coastal erosion rates currently being experienced at all three study areas (Fletcher et al. 2013). The first organisms to be impacted by SLR include the endangered monk seals that require beaches for resting, and molting (Baker et al. 2006) and the sea turtles (e.g. green sea turtle and endangered hawksbill turtle) that require beaches for nesting (Fuentes and Cinner 2010). Intertidal habitats also serve as important staging sites where migrant shorebirds can feed and rest and the loss of such sites can cause severe ‘bottleneck’ effects on migratory populations (Iwamura et al. 2013). As sea-level continues to rise, beaches will naturally migrate landwards unless prevented by structures such as roads, home lots, etc. (Fish et al. 2008). James Campbell is the only study area without any coastal structures and by facilitating cross-shore movement of beach habitats, endangered and threatened organisms may be preserved during the slow phase.

In addition to managing current impacts of the slow phase of flooding, wetland managers will also be challenged to create future adaptive management strategies to plan for the fast phase of flooding. As SLR transitions into the fast phase, flooding along the beaches will begin to encroach landward as both marine and groundwater elevations rise. To preserve inland wetland habitats, wetlands will need to be pumped more frequently to maintain low water levels. Increased salinity by groundwater intrusion may also cause more salt tolerant vegetation to replace the native plants required by water birds for food, foraging, and the construction of nests.

In all 3 study areas, the timeframe by which intensive management can aid in the preservation of coastal habitats is limited. Wetland mitigation sites will need to be identified both within and potentially outside of current wetland refuge boundaries. Making these decisions, in the context of specific timeframes of vulnerability, may enhance the capacity of stakeholders to create management plans that increase the resiliency of systems and support the ability of natural systems to adapt to change.

Conclusions

Characterizing flooding into slow and fast phases provides decision-makers with a locally based time frame to implement plans to manage the largest impacts of SLR. As time progresses and the fast phase of flooding approaches, the risk associated with delayed decision-making increases. The SLR vulnerability maps created in this study can be used as a guide to identify threatened areas and initiate decision making that benefits both wetland and coastal strand environments, and the neighboring community. By assessing the joint uncertainty of both datasets used in this study, wetland managers can refine their definition of threatened areas based upon the probability that an area will be vulnerable to SLR impacts at a particular time. The methodology provided in this study is applicable to not only Hawai‘i but also all other low-lying coastal areas.

CHAPTER 3

MODELING SEA-LEVEL RISE VULNERABILITY OF COASTAL WETLANDS USING RANKED MANAGEMENT CONCERNS

Haunani H. Kane, Charles H. Fletcher, L. Neil Frazer, Tiffany Anderson, and Matthew M. Barbee

Abstract

Coastal strand and wetland habitats are intensively managed to restore and maintain populations of endangered species. However, sea-level rise threatens the work of resource managers because coastal erosion, salt-water intrusion, and flooding degrade critical habitats. Because habitat loss is a measure of the risk of extinction, managers are keen to receive guidelines and other tools to reduce the risk posed by sea-level rise. Improving upon standard inundation mapping techniques we develop a ranking system that models sea-level rise vulnerability as a function of six input parameters defined by wetland experts: type of inundation, time of inundation, soil type, habitat value, infrastructure, and coastal erosion. To exemplify the method, the model is applied to three coastal wetlands on the Hawaiian islands of Maui and O‘ahu. Each ranked input parameter is mapped upon a 2 m horizontal resolution raster and final vulnerability is obtained by calculating the weighted geometric mean of the input vulnerability scores. Areas that ranked with the ‘highest’ vulnerability should be the focus of future management efforts. The tools developed in this study can be used as a guide to prioritize conservation actions at flooded areas and initiate decisions to adaptively manage sea-level rise impacts.

Introduction

Globally, coastal strand and wetland habitats have high conservation value due to the role they play in the preservation of endangered and endemic organisms. Wetlands provide a variety of functions that reduce storm damage and stabilize shorelines (Gedan et al. 2011), trap land-based sediments, retain nutrients, and alleviate flooding (Bruland 2008). In the Pacific region alone, over 2,500 islands and atolls harbor a diverse range of freshwater, coastal, and marine wetlands (Ellison 2009). It has been noted that the disappearance of small wetlands will cause a dire reduction in the ecological connection among remaining species populations (Semlitsch & Bodie 1998).

SLR is a growing problem on low lying coastal plains and threatens costal strand and wetland habitats with increased erosion (Romine et al. 2013), frequency of extreme high water events (Tebaldi et al. 2012), pond water levels, and salinity. The Intergovernmental Panel on Climate Change (IPCC) Fifth Assessment Report predicts under a worst case (RCP8.5) scenario, global sea-level for the year 2100 is likely to increase to 0.53 to 0.98 m relative to 1986-2005 (Church et al. 2013). Variability in global mean sea-level has been modeled and the greatest amplitude in SLR is predicted for the tropical Pacific (Slangen et al. 2012; Spada et al. 2013). Islands within the tropics are especially vulnerable because species have narrow tolerances for changes in climate (Mora et al. 2013), and microtidal (< 2 m tidal range) environments do not allow for large concentrations of marine suspended sediment to aid in vertical accretion in response to SLR (Kirwan et al. 2010).

To date, the majority of insular SLR vulnerability research has focused on summarizing impacts on a global sclale (e.g. Wetzel et al. 2012; Bellard et al. 2013). For example, Bellard et al. (2013) found that approximately 6% of the 4,447 islands investigated worldwide would be entirely submerged under 1 m of SLR. Global assessments are beneficial for demonstrating the general consequences of SLR, however through the use of low resolution elevation data sets, the final vulnerability maps are produced with large errors (Cooper et al. 2013b). Furthermore most management occurs at regional and local scales, thus fine-scale vulnerability assessments are more relevant for direct decision making (Halpern et al. 2007).

Prior regional scale assessments have defined SLR vulnerability based upon high-resolution elevation alone (e.g. Gesch 2009; Cooper et al. 2013a) or as a balance between vertical accretion potential and the changing rate of SLR (e.g. Kirwan & Temmerman 2009; Kirwan et al. 2010; Morris et al. 2011). However within highly managed areas, landscape vulnerability is related to the site-specific goals of decision makers. In this study we build upon past research that couples the use of a geographic information system (GIS) and expert elicitation (e.g. Van Lonkhuyzen et al. 2004; White and Fennessy 2005) to systematically rank and map SLR vulnerability at three Hawaiian wetlands that are representative of numerous small wetlands from across the 2,500 islands in the Pacific. We develop a method to prioritize management strategies in response to SLR based upon a number of predetermined factors such as the time and nature of flooding, environmental features that influence flood severity, and the loss that would result from flooded high value habitats and infrastructure. The vulnerability ranking process may be easily refined and replicated to other small, microtidal islands to accommodate different planning needs, data availability, and sources of expert knowledge.

Methods

The modeling approach used in this study to assess SLR vulnerability is outlined in Figure 3.1. Study sites were identified based upon the biological integrity of managed resources within an area, the existence of experienced and knowledgeable management staff, and the availability of mappable layers such as high resolution topographic data (Figure 3.1a). We defined vulnerability from a management perspective by mapping those parameters that best characterize how SLR will impact decision makers' ability to accomplish mandated goals and objectives (Figure 3.1b). Data availability, professional judgement, and elicited expert knowledge were used to rank vulnerability parameters for each study site from very high (5) to very low (1) (Figure 3.1c). We used a GIS to apply the ranked vulnerability scores and applied a weighted geometric mean to map the cumulative vulnerability (Figure 3.1d-f). Areas with the highest vulnerability were identified and should be used to guide adaptive management planning (Figure 3.1g-h). Wetland experts may modify the model and refine the definition of vulnerability as new information becomes available (Figure 3.1i).

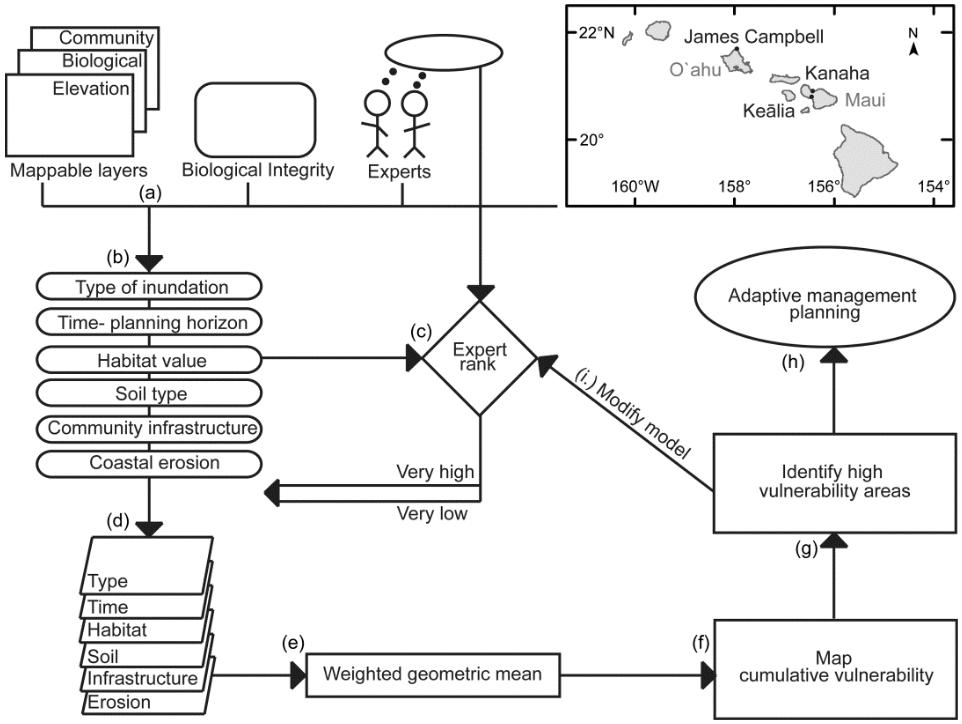

Figure 3.1. Depiction of the vulnerability ranking process.

Study area

In conjunction with the Hawaiʻi Wetland Joint Venture, a group that represents state, federal, and local wetland managers, three coastal wetland environments were identified for this study: James Campbell National Wildlife Refuge (north Oʻahu), Kanaha Pond State Wildlife Sanctuary (north Maui), and Keālia Pond National Wildlife Refuge (south Maui). All three study sites represent areas of high biodiversity and endemism, and are strategically managed to provide habitats for the recovery of endangered waterbirds, the endangered Hawaiian monk seal (*Monachus schauinslandi*), the threatened Hawaiian green sea turtle (*Chelonia mydas*), seabirds, and migratory shorebirds. One to two senior wetland experts were identified at each study site. Wetland experts were comprised of wetland managers who from training, research, and personal experience (5-20+ years) possess the greatest capacity to assess how SLR will impact future management strategies.

Defining SLR vulnerability

Primarily, natural resource managers are concerned with prioritizing management at flooded areas based upon the value of each site. Three primary vulnerability parameters referred to as type of inundation, time of inundation, and habitat value were identified and should be used in all applications of this methodology. The type of inundation parameter compared a wetland manager's ability to manage impacts due to marine inundation (surface flooding from the ocean), and groundwater inundation (associated with rising water tables). The time of inundation parameter assessed the wetland manager's planning horizon or his ability to create and employ long-term adaptive management strategies in response to impacts. The habitat value parameter created an inventory of the emphasis that is placed upon the management of key species within coastal strand, wetland, and upland habitats.

Secondary vulnerability parameters refine the definition of threatened resources based upon the availability of additional data such as soil type, community infrastructure, and coastal erosion hazard zones. Soil type was used to identify poor draining, high salinity, hydric soils that may act as ponding areas for floodwaters. The infrastructure parameter was used to identify regions within the managed bounds that if inundated, may flood surrounding community infrastructure. The coastal erosion parameter modeled the landward migration of future shorelines under elevated sea-level.

Ranking SLR vulnerability parameters

Expert judgment was utilized in a structured manner to rank primary vulnerability parameters. Face to face surveys were conducted and experts were asked a series of questions pertaining to the three primary input parameters; time of inundation, type of inundation, and habitat value. Experts ranked the vulnerability of their refuge to SLR from very low (1) to very high (5) (Table 3.1). After each survey question respondents were asked to indicate how confident they were about the depth of knowledge used to determine vulnerability (Halpern et al. 2007; Selkoe et al. 2008; Fuentes & Cinner 2010). Confidence values ranged from very low (1) to very high confidence (5). In the case of multiple respondents for each study site, a weighted confidence approach was used, such that expert rankings made with higher confidence were weighted higher than low confidence responses (Equation 3.1) (Halpern et al. 2007).

$$\text{Vulnerability Input Rank} = \frac{\sum \text{Vulnerability Score} \times \text{Confidence}}{\sum \text{Confidence}} \tag{3.1}$$

Secondary input parameters were ranked based upon the presence of poor draining hydric soils, infrastructure, and coastal erosion. Sites within each study area were assigned a very high vulnerability rank if secondary input parameters were present and very low vulnerability if secondary parameters were not present.

Table 3.1. SLR vulnerability ranked from very low (1) to very high (5) for each of the six input parameters.

Parameter	Weight	James Campbell	Keālia	Kanaha
Type of inundation	2			
Groundwater		5	4	4
Marine		4	5	4
Not inundated		1	1	1
Time of inundation	2			
2057 (0.30 m)		2	4	3
2100 (0.74 m)		3	4	5
Not inundated		1	1	1
Habitat value	2			
Coastal strand		4	3	2
Upland shrub/forest		2	2	3
Wetlands		5	5	5
Soil type	1			
Hydric		3	3	*None
Non-hydric		1	1	
Community infrastructure	1			
3 types		5	5	5
2 types		4	4	4
1 type		3	3	3
None		1	1	1
Coastal erosion	1			
Erosion hazard		5	5	5
Hardened shoreline		3	*None	3
None		1	1	1

*Hydric soils or hardened shorelines were not found at these study areas.

Mapping SLR vulnerability

GIS layers for each input parameter were compiled, and 2 m horizontal resolution rasters were produced such that each cell represented a corresponding vulnerability rank (Table 3.1). To map type and time of inundation, SLR inundation maps were interpolated from LiDAR digital elevation models (DEMs) with 2 m horizontal resolution, and 0.18-0.20 m (1 σ) vertical accuracy. To assess the percent probability that a location is inundated we accounted for the uncertainty of the LiDAR data and the SLR model. The IPCC's fifth assessment report (AR5) Representative Concentration Pathways 8.5 (RCP8.5) model provides yearly mean sea-level and associated uncertainty (1 σ) values up until the year 2100. A cumulative percent probability approach, similar to NOAA (2010) and Mitsova and Li (2012) was used to calculate a standard-score (SS_{xy}) or the number of standard deviations a value differs from the mean.

$$SS_{xy} = \frac{\mu_s - \mu_z}{\sqrt{\sigma_s^2 + \sigma_z^2}} \tag{3.2}$$

The standard-score was calculated through a cell by cell approach where the difference between the projected sea-level value above MHHW (μ_s) and the DEM elevation (μ_z) was divided by the joint-uncertainty of SLR projections (σ_s) and LiDAR data (σ_z). The standard score was converted to a percent probability via a look-up table. At each point in the low confidence area for a particular time the probability of flooding is 50%, and at each point in the high confidence area the probability of flooding is 80%. The high confidence area is thus a subset of the low confidence area.

One of the key issues for managing wetlands is identifying which areas may be impacted by marine (salty) inundation or groundwater (potentially fresh or brackish) inundation as waterfowl and vegetation are sensitive to both increased pond water levels and salinity (U.S. Fish and Wildlife Service 2011a, 2011b). Areas of marine inundation were identified at a specified SLR scenario by isolating DEM cells that are hydrologically connected to the ocean or adjacent flooded cells as determined by the 8-sided hydrologic connectivity method (Cooper et al. 2013b). Inundated areas disconnected from the ocean were assumed to be flooded by rising groundwater levels (Rotzoll & Fletcher 2012). Wetland experts ranked the vulnerability of their study area to both types of inundation by considering natural and constructed features that may impede future surface inundation, as well as their dependency upon groundwater sources to maintain pond water levels.

The ability of highly managed ecosystems to successfully adapt to SLR lies in the capacity of coastal decision makers to develop and implement long-term adaptive management plans. The time of inundation parameter ranked wetland managers' ability to implement strategies to manage 0.30 m of SLR by 2057, and 0.74 m of SLR by 2100. IPCC 's RCP8.5 SLR model was used to correlate sea-level heights with time (Church et al. 2013). A low ability to plan for a specific time period corresponds to a high vulnerability to SLR impacts.

To assess the ecological value of coastal sites that may potentially be flooded by SLR, experts were asked to rank the emphasis that is placed upon the management of a list of predetermined species within mapped coastal strand, wetland, and upland habitats. Managed areas that have a high habitat value were ranked highly vulnerable to SLR because these areas will result in the greatest loss in endangered and native organisms if impacted by SLR. For example, globally coastal strand habitats are managed to support important nesting sites for sea turtles (Fuentes & Cinner 2010), resting areas for monk seals (Baker et al. 2006), and winter staging sites for migrant shorebirds (Galbraith et al. 2002). In addition coastal dune plants stabilize dunes and if lost will lead to an increase in erosion exacerbating habitat loss (Feagin et al. 2005). Wetland areas delineated by the National Wetlands Inventory (http://www.fws.gov/wetlands/Data/Mapper.html) are managed primarily to provide habitat for Hawai‘i’s four endemic and endangered waterbirds. Upland habitats are defined as the non-wetland or coastal strand area.

The presence of hydric soils is one of the primary indicators used to identify the occurrence of historical wetlands, as well as potential areas to support the establishment of future wetland ecosystems (Richardson & Gatti 1999; Van Lonkhuyzen et al. 2004; White and Fennessy 2005). Poorly drained and moderately to strongly saline hydric soil types were identified in each study area using soil maps derived from the Natural Resource Conservation Service (NRCS) web soil survey (http://websoilsurvey.nrcs.usda.gov/app/). Hydric soils included Kealia silt loam, Kaloko clay, Keaau clay, and Pearl Harbor clay. Due to their low draining potential of hydric soils, we assumed that areas with hydric soils are very highly vulnerable to prolonged flooding, whereas non-hydric soil areas have a very low vulnerability.

Coastal and wetland managers have a commitment to mitigate flood impacts upon both refuge and surrounding community infrastructure (U.S. Fish and Wildlife service 2011a, 2011b). To assess the proximity of flooded areas to infrastructure, we mapped a 50 m buffer around three infrastructure types including roads, 2010 U.S. census designated urban areas (http://planning.hawaii.gov/gis/ download-gis-data/), and rural areas such as defined by the National Oceanic and Atmospheric Administration (NOAA) Coastal Change Analysis Program (CCAP) (http://www.csc.noaa.gov/digitalcoast/ data/ccapregional). Rural areas included developed open space (e.g. golf courses, and rural house lots), cultivated land (e.g. agriculture, and aquaculture facilities), and impervious surfaces (e.g. houses, and buildings). Flooded areas that intersect buffered infrastructure were ranked very highly vulnerable because refuge flooding may impact the nearby community.

SLR threatens beaches and dunes with chronic erosion and causes a landward displacement of coastal environments (Feagin et al. 2005). We modeled the effects of accelerated SLR using a hybrid model that combined the change in shoreline positions due to future sea-level predicted by the Bruun rule (Bruun 1962), with historical shoreline change data collected by the University of Hawai‘i Coastal Geology Group (Fletcher et al. 2013). Mapped erosion hazard zones encompass the area occupied between the current shoreline and the future shoreline position predicted under a 0.74 m rise in sea-level at the year 2100. Hazard zones projected from sandy shorelines are ranked very highly vulnerable to SLR, while those projected from hardened shorelines are ranked moderately vulnerable.

Identifying high vulnerability areas

Once each of the individual vulnerability parameters were ranked (Table 3.1) and mapped (Figure 3.2a-f), cumulative vulnerability was determined. The final spatial variation of vulnerability for each study area was found by combining the individual vulnerability parameter rasters using a weighted geometric mean (Equation 3.3).

$$\text{Final Vulnerability} = (\text{type}^2 \times \text{time}^2 \times \text{habitat}^2 \times \text{soil} \times \text{infrastructure} \times \text{erosion})^{\frac{1}{9}} \tag{3.3}$$

Assigning weights to input parameters allows one to account for the relative importance of each parameter in determining SLR vulnerability. This approach is mathematically similar to the wetland suitability modeling methodology used by Van Lonkhyzen et al. (2004). Primary input parameters (type, time, and habitat) were ranked higher than secondary parameters (soil, infrastructure, and erosion) because the primary input parameters most directly reflect manager’s goals and objectives.

Results and Discussion

Increases in pond water height and salinity directly impact managers’ ability to provide suitable habitat for endangered waterbirds. We found that groundwater inundation represents over 90% of the total inundation at all three study areas (Table 3.2). Sand dunes act as a natural buffer to the ocean and inhibit marine inundation from entering the interior wetlands. However, as sea-level increases beyond 0.74 m, marine water may begin to breech narrow outlet ditches, dikes, and other low lying features and could potentially shift the dominant source of inundation to marine inundation.

Table 3.2. Percent area impacted by type and time of inundation under the RCP8.5 scenario.

Type of inundation				
	High confidence (P>80%)		Low confidence (P>50%)	
Study Area	% Area	% Total inundation	% Area	% Total inundation
James Campbell				
Groundwater	1.4	93.2	9.6	97.4
Marine	0.1	6.8	0.3	2.6
Kanaha				
Groundwater	25	46	29.4	98.9
Marine	29.4	54	0.3	1.1
Keālia				
Groundwater	27.6	98	39.2	98.1
Marine	0.6	2	0.8	1.9
Time of inundation				
	High confidence (P>80%)		Low confidence (P>50%)	
Study Area	% Area	% Total inundation	% Area	% Total inundation
James Campbell				
2057 (0.30 m)	0.1	5.3	0.7	7.5
2100 (0.74 m)	1.5	94.7	9.1	92.5
Kanaha				
2057	24.9	98.7	25.1	84.5
2100	0.3	1.3	4.6	15.5
Keālia				
2057	21.9	77.7	25.3	63.3
2100	6.3	22.3	14.7	36.7

Survey responses from wetland experts varied when asked to rank their future ability to manage both marine and groundwater impacts. At James Campbell, wetland managers believed it would be more difficult to pump wetlands to alleviate increased groundwater inputs, while at Keālia, salty hydric soils are currently impacting waterbirds and vegetation. The wetland manager at Kanaha expressed concerns about groundwater inundation; however both types of flooding were ranked as highly vulnerable.

Wetland managers were asked to consider their ability to manage mid and end of the century impacts according the RCP8.5 SLR projections. Most long-term conservation plans, however, are based upon shorter time scales, and wetland experts stated that they do not typically plan beyond 15 years into the future. Our analysis revealed that the bulk of inundation at James Campbell (94.7% of surface area) is projected to occur in the second half of the century (Table 3.2). This coincides with a time period when wetland managers believe they are most vulnerable to SLR. At Keālia and Kanaha large seasonal wetlands will expand and experience increased pond depth in the second half of the century.

Mapped wetland habitat types were found to be the most important habitats due to the role that they play in the preservation of endangered waterbirds, and were ranked highly vulnerable to SLR. At James Campbell and Keālia, coastal strand habitats ranked second based upon the priority each refuge gives to the management of native coastal plants, the monk seal, and sea turtles. At Kanaha, upland habitats are valued as potential sites to relocate wetland habitats.

Poor draining, high salinity, hydric soils occupy relatively large areas at James Campbell and Keālia. The hydric soil layer at these two study areas includes both existing wetlands and surrounding upland areas which may in the future be prone to long periods of standing water due to poorly drained soils. Kahana was the only study area that lacked hydric soils.

On the basis of infrastructure alone, the areas of the highest vulnerability are located near refuge infrastructure or along the refuge boundaries that are bordered by community infrastructure. As the number of community infrastructure types increases there is a greater risk that flooding within the refuge will impact bordering roads, urban, and rural communities. This is especially true at Kanaha, which is located an urban area and is completely surrounded by development. Accounting for land and building values in Kahului, an independent study by Cooper et al. (2013a) found that a 0.75 m rise in sea-level would result in a loss of $18.7 million dollars. At Keālia the majority of infrastructure is located on the narrow coastal strip and is bordered on both sides by inundation.

All three study areas are currently experiencing chronic coastal erosion (Fletcher et al. 2013). Two out of the three study areas have roads, houses and other developed structures that will prevent the natural landward migration of beaches as sea-level rises. Coastal squeeze may significantly alter the future availability of coastal habitats (Clausen & Clausen 2014).

Composite vulnerability scores were compiled and the areas with the highest vulnerability rank were identified. At all three study areas the dominant factor in determining vulnerability is whether or not an area is inundated, which is an artifact of the weighting scheme that was applied. Wetland managers, however, may find it useful to prioritize management efforts at flooded areas and thus the other input parameters were applied. Keālia most successfully exemplifies the applicability of this methodology. Figure 3.2g illustrates both the areas predicted to be inundated by 2100 (blue) as well as a subset of the inundated areas that ranked a higher vulnerability (yellow and red). Referring to our input vulnerability maps (Figure 3.2a-f), the areas of highest vulnerability are defined as inundated hydric soil wetlands and the eroded coastal strand that fall within 50 m of infrastructure. At Keālia, infrastructure serves as the distinguishing feature in determining high vulnerability, as the majority of the flooded area encompasses wetlands habitat and hydric soils. At Kanaha high vulnerability areas are defined as inundated wetlands, uplands and coastal stand habitats that fall within the erosion hazard zone (Figure 3.3). High vulnerability areas at Kanaha mirror the areas inundated at 0.74 m. High vulnerability areas at James Campbell are defined as inundated coastal strand environments within the erosion hazard zone, and inundated wetlands with hydric soil (Figure 3.4).

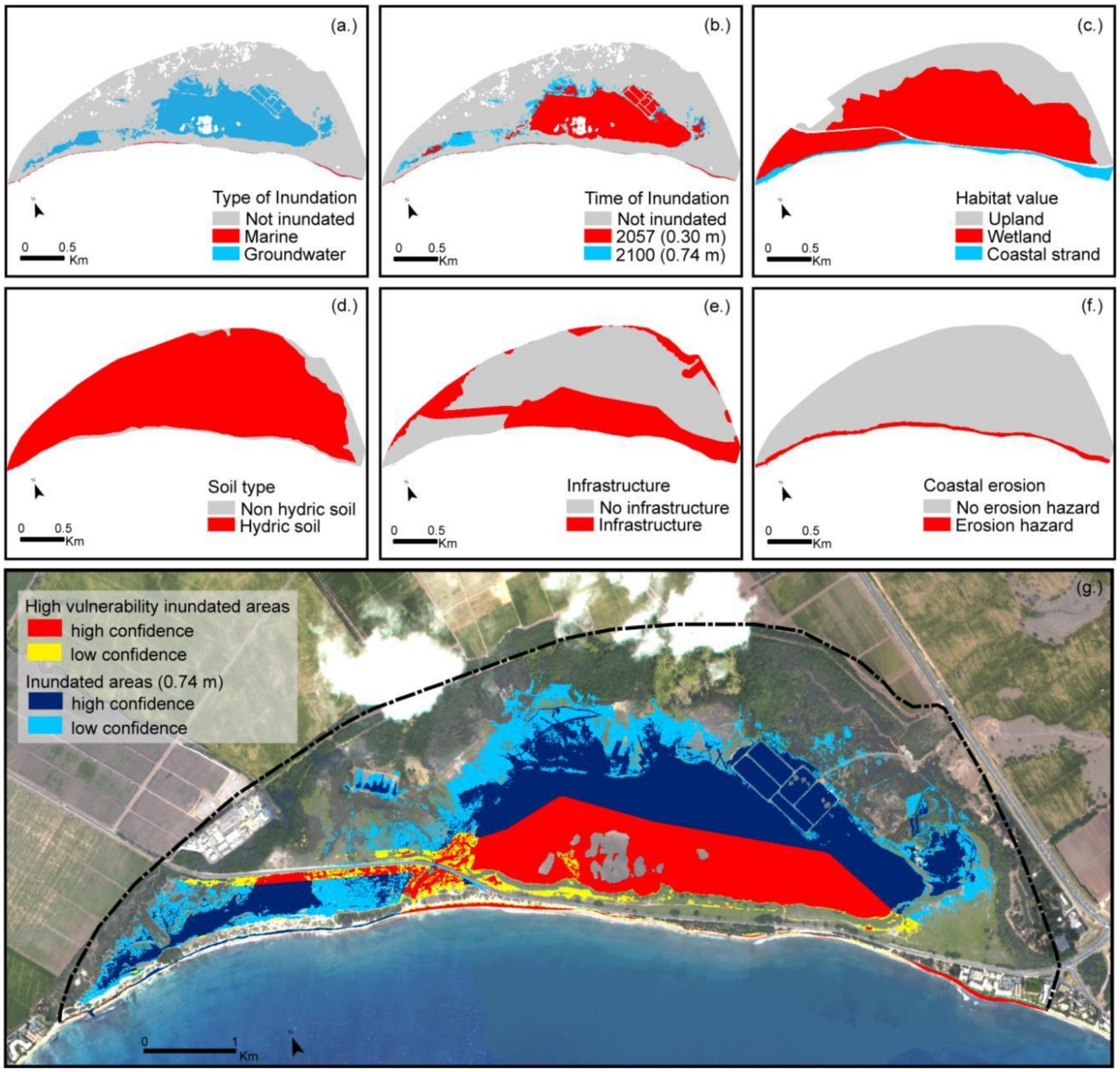

Figure 3.2. Example vulnerability maps for Keālia National Wildlife Refuge. Vulnerability is defined and high confidence areas (80 % probability of flooding) are mapped for six input parameters; type of inundation (a), time of inundation (b), habitat value (c), soil type (d), infrastructure (e), and coastal erosion (f). Input parameter vulnerability maps are combined (g) and areas of the highest vulnerability (red and yellow) are identified as a subset of the total area inundated at 0.74 m by 2100 (blue). High vulnerability areas are mapped at high (80% probability of flooding) and low confidence (50%).

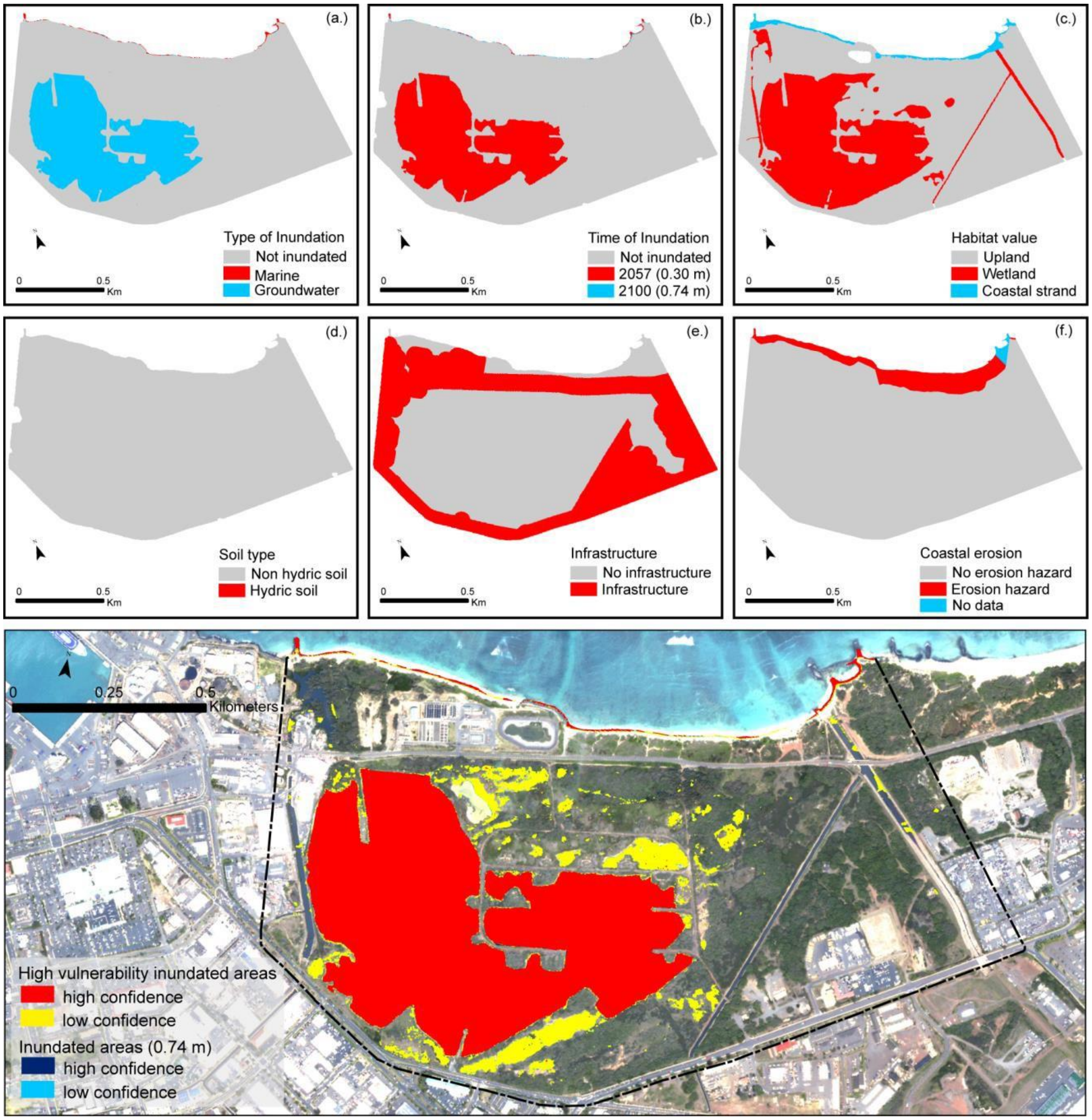

Figure 3.3 Example vulnerability maps for Kanaha State Wildlife Refuge. Vulnerability is defined and high confidence areas (80 % probability of flooding) are mapped for six input parameters; type of inundation (a), time of inundation (b), habitat value (c), soil type (d), infrastructure (e), and coastal erosion (f). Input parameter vulnerability maps are combined (g) and areas of the highest vulnerability (red and yellow) are identified as a subset of the total area inundated at 0.74 m by 2100 (blue). High vulnerability areas are mapped at high (80% probability of flooding) and low confidence (50%).

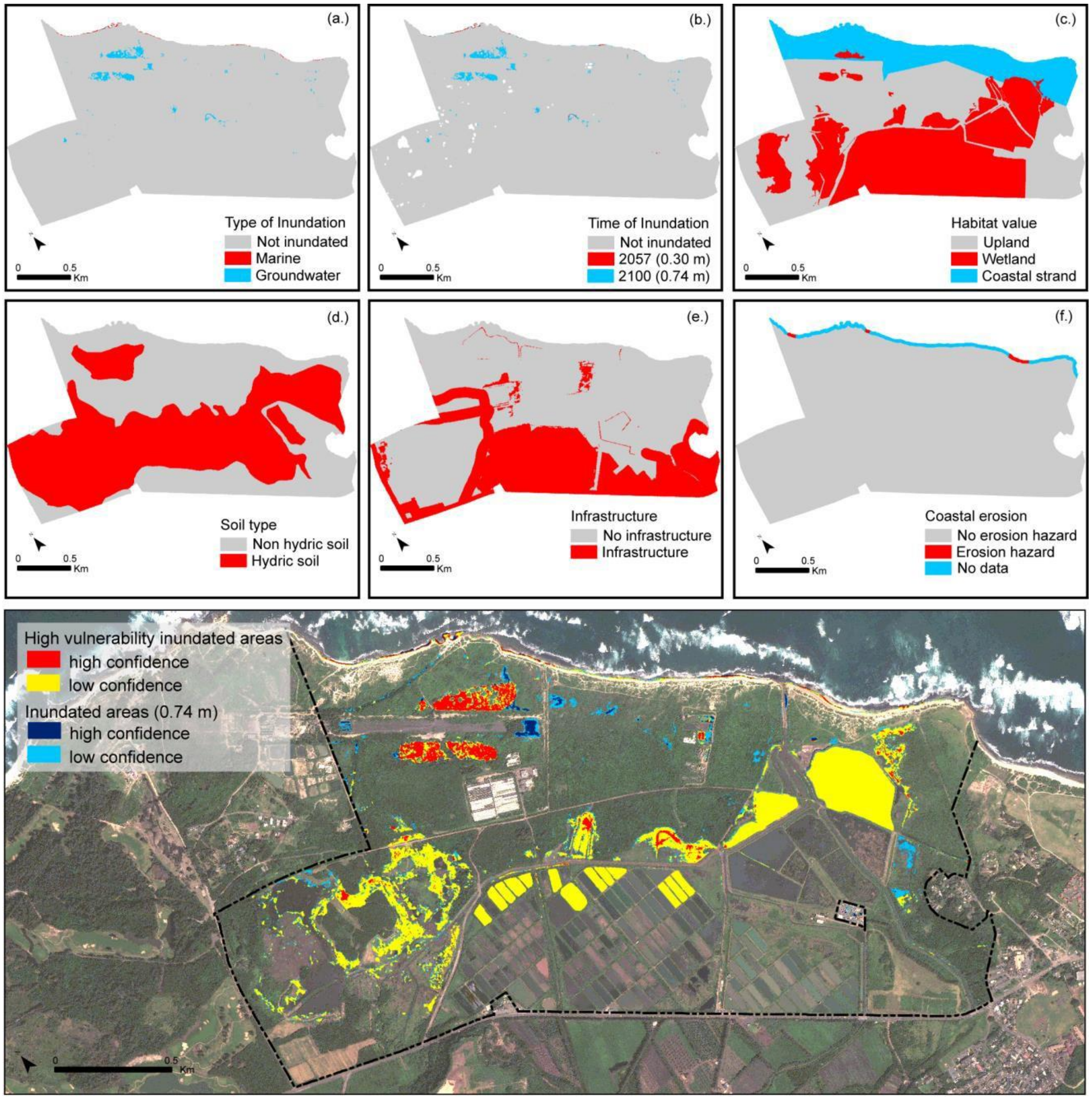

Figure 3.4. Example vulnerability maps for James Campbell National Wildlife Refuge. Vulnerability is defined and high confidence areas (80 % probability of flooding) are mapped for six input parameters; type of inundation (a), time of inundation (b), habitat value (c), soil type (d), infrastructure (e), and coastal erosion (f). Input parameter vulnerability maps are combined (g) and areas of the highest vulnerability (red and yellow) are identified as a subset of the total area inundated at 0.74 m by 2100 (blue). High vulnerability areas are mapped at high (80% probability of flooding) and low confidence (50%).

Conclusions

Under changing climate conditions it will be increasingly difficult to achieve all conservation objectives for habitats, species and protected areas (Hossell et al. 2003).

The greatest challenge will be prioritizing management actions in response to impacts. A number of studies have developed vulnerability-ranking processes where threats with the greatest impact are assigned the highest priority and dealt with first (e.g. Halpern et al. 2007; Selkoe et al. 2008; Fuentes & Cinner 2010). To date, the majority of insular SLR assessments have focused on global impacts; however there is a need for finer scale analysis because most management happens at a regional or local scale. This study is unique in that it couples expert knowledge and empirical data to define and map input parameters that systematically rank SLR vulnerability.

The method used here translates the ranking process into a series of maps that identify high vulnerability areas where adaptive management efforts are needed most. The entirety of this process should encourage discussion of how managing high priority or high vulnerability areas will impact current management objectives and goals. For example coastal decision makers should identify low lying areas and discuss how management of these areas may be impacted by marine and groundwater sources of flooding. Creating an inventory of infrastructure, valued habitats, and cultural assets that fall within the predicted areas of flooding may assist in prioritizing which flooded habitats to manage first. Conservation strategies most likely will need to be updated to meet the challenges of future SLR impacts. Management will need to determine which areas can be preserved, or relocated, and some areas may need to be abandoned. In the case of urban wetlands, high vulnerability flooded areas will require continuous maintenance to alleviate flooding of the surrounding community.

We acknowledge that various management groups or regions have different goals and objectives. The strength of this approach is that the rankings as well as the input parameters and data can be updated to include new sources of information and refine results from this analysis. We recommend that the primary input parameters be employed in all aspects of this methodology, however the secondary vulnerability parameters are interchangeable and can be altered to reflect the availability of data and needs of the user. It is important to note that the quality of model output is a function of the quality of input data, and expert knowledge. Vertical error of a DEM has the largest influence on defining areas of inundation (Zhang 2011), and it is recommended that LiDAR data be used by decision makers to identify high-resolution hazard zones (Cooper et al. 2013b).

The expert knowledge elicitation process greatly benefits from face-to-face surveys that allow input parameters to be adequately defined or updated so that they are truly beneficial in determining rank. This process encourages decision makers to feel more confident in focusing resources to manage these 'high vulnerability' areas because of the integral role they play in identifying and ranking each of the vulnerability input parameters. Our study employed a small sample size due to limited management staff at each study site. Rather than consulting a larger group of experts who may have a general idea of how each coastal ecosystem functions, wetland managers found it more beneficial to sample a smaller number of experts who have in-depth knowledge of site specific characteristics, historical factors, and management goals of each wetland.

The greatest gap in knowledge arose when defining long-term plans from the perspective of climate science models and wetland experts. SLR is a relatively slow process, and the majority of impacts, with the exception of seasonally flooded wetlands, are predicted and modeled for the second half of the century. Wetland experts cite the U.S. Fish and Wildlife Service Comprehensive Conservation Plans as the extent of current long-term planning. These documents provide specific management guidance for each national wildlife refuge system over a period of 15 years (e.g. U.S. Fish and Wildlife Service 2011a, 2011b). Wetland experts attributed their limited ability to plan further into the future to the uncertainty in future funding, limited staff coupled with a high number of daily responsibilities and the lack of pressure in the past to plan for longer time periods. There is a great need to extend the planning horizon of wetland resource managers and to improve SLR modeling and mapping products. Encouraging scientists and managers to work closely together may ensure that scientific products are relevant to their use in decision making.

REFERENCES CITED

Baker J D, Littnan C L, Johnston D W (2006) Potential effects of sea level rise on the terrestrial habitats of endangered and endemic megafauna in the Northwestern Hawaiian Islands. Endangered Species Research 2:21-30

Bamber J L, Aspinall W P (2013) An expert judgement assessment of future sea level rise from the ice sheets. Nature Climate Change 3:424-427

Bjerklie D M, Mullaney J R, Stone J R, Skinner B J, Ramlow M A (2012). Preliminary investigation of the effects of sea-level rise on groundwater levels in New Haven, Connecticut: U.S. Geological Survey Open-File Report 2012–1025, 46 p., at http://pubs.usgs.gov/of/2012/1025/.

Bellard C, Lederc C, and Courchamp F (2013) Impact of sea level rise on the 10 insular biodiversity hotspots. Global Ecology Biogeography 23:203-212

Bruland, G L (2008) Coastal wetlands: Function and role in reducing impact of land-based management. In: Fares A, El-Kadi A I (ed) Coastal Watershed Management. WIT Press, Southhampton, UK, pp 85-124

Bruun, P (1962) Sea level rise as a cause of shoreline erosion. Am. Soc. Civ. Eng. Proc., J. Waterways Harbors Div. 88:117-130

Caccamise D J, Merrifield M A, Bevis M, Foster J, Firing Y, Schenewerk M., Taylor F, Thomas D (2005) Sea level rise at Honolulu and Hilo, Hawaii: GPS estimates of differential land motion. Geophysical Research Letters 32, L03607

Church J A, White NJ (2011) Sea-Level Rise from the Late 19th to the Early 21st. Century Surveys in Geophysics 32;585-602.

Church, J.A., et al. 2013. Sea Level Change. In: *Climate change 2013: The Physical Science Basis. Contribution of Working Group 1 to the Fifth Assessment of the Intergovernmental Panel on Climate Change*. [Stocker, T.F., D. Qin, G. –K Plattner, M. Tignor, S. K. Allen, J. Boschung, A. Nauels, Y. Xia, V. Bex and P. M. Midgley (eds)]. Cambridge University Press, Cambridge, United Kingdom and New York, NY, USA

Clausen K K, Clausen P (2014) Forecasting future drowning of coastal waterbird habitats reveals a major conservation concern. Biological Conservation 171: 177-185

Cooper H, Chen Q, Fletcher C H, Barbee M M (2013a) Assessing vulnerability to sea-level rise in Maui, Hawaiʻi using LiDAR remote sensing and GIS. Climatic Change 116:547-563

Cooper H M, Chen Q, Fletcher C H, Barbee M (2013b) Sea-level rise vulnerability mapping for adaptation decisions using LiDAR DEMs. Progress in Physical Geography. DOI: 10.1177/0309133313496835

Dewberry (2008) *LiDAR QAQC Report Hawaii TO12: Molokai, Maui, Lanai Islands March 2008* (Fairfax, Virginia: Dewberry)

Dobson A P, Rodriguez W M, Wilcove D S (1997) Geographic distribution of endangered species in the United States. Science 275:550-553

Ellison JC (2009) Wetlands of the Pacific Island region. Wetland Ecology Management 17: 169-206

Feagin R A, Sherman D J, Grant W E (2005) Coastal erosion, global sea-level rise, and the loss of sand dune plant habitats. Frontiers in Ecology and the Environment 3:359-364

FGDC, 1998. *Geospatial positioning accuracy standards, Part 3. national Standard for Spatial Data Accuracy* (http://www.fgdc.gov/standards/projects/FGDC-standards-projects /accuracy/part3/index_html, accessed July 2012)
Fish M R, Cote I M, Horrocks J A, Mulligan B, Watkinson A R, Jones A R (2008) Construction setback regulations and sea-level rise: Mitigating sea turtle nesting beach loss. Ocean and Coastal Management. 51:330-341
Fletcher C, Rooney J, Barbee M, Lim S-C, Richmond BM (2003) Mapping shoreline change using digital orthophotogeometry on Maui, Hawaii. Journal of Coastal Research SI38:106-124
Fletcher C H, B M Romine B M, Genz A S, Barbee M M, Dyer M, Anderson T R, Lim S C, Vitousek S, Bochicchio C, Richmond B M (2013) National Assessment of Shoreline Change: Historical Shoreline Change in the Hawaiian Islands: U.S. Geological Survey Open-File Report 2011-1051, 55 p. (http:pubs.usgs.gov/of/2011/1051)
Fuentes, M M P B, Cinner J E (2010) Using expert opinion to prioritize impacts of climate change on sea turtles. Journal of Environtal Management 9:2511-2518
Galbraith H, Jones R, Park R, Clough J, Herrod-Julius S, Harrington B, Page G (2002) Global Climate Change and Sea Level Rise: Potential Losses of Intertidal Habitat for Shorebirds. Waterbirds 25:173-183
Gardner A S, Moholdt G, Cogley J G, Wouters B, Arendt A A, Wahr J, Berthier E, Hock R, Pfeffer W T, Kaser G, Ligtenberg S R M, Bolch T, Sharp M J, Hagen J O, van den Broeke M R, Paul F (2013) A Reconciled Estimate of Glacier Contributions to Sea Level Rise: 2003 to 2009. Science 340:852-857
Gedan K B, Kirwan M L, Wolanski E, Barbier E B, Silliman B R (2011) The present and future role of coastal wetland vegetation in protecting shorelines: answering recent challenges to the paradigim. Climatic Change 106:7-29
Gesch D B (2009) Analysis of Lidar Elevation Data for Improved Identification and Delineation of Lands Vulnerable to Sea-Level Rise. Journal of Coastal Research SI53:49-58
Halpern B S, Selkoe K A, Fiorenza M, Kappel C V (2007) Evaluating and ranking vulnerability of global marine ecosystems to anthropogenic threats. Conservation Biology 21:1301-1315
Horton B P, Rahmstorf S, Engelhart S E, Kemp A C (2014) Expert assessment of sea-level rise by AD 2100 and AD 2300. Quaternary Science Reviews 84: 1-6.
Hossell J E, Ellis N E, Harley M J, Hepburn I R (2003) Climate change and nature conservation: Implications for policy and practice in Britain and Ireland. Journal for Nature Conservation 11:67-73
Hunt C, De Carlo E (2000) Hydrology and Water and Sediment Quality at James Campbell National Wildlife Refuge Near Kahuku, Island of Oahu, Hawaii. Available on-line at: http://pubs.usgs. gov/wri/wri99-4171/pdf/wri99-4171.pdf.
Intergovernmental Panel on Climate Change (IPCC) (2007) Climate Change 2007- the physical science basis. In: Solomon, S., Qin, D., Manning, M., Chen, Z., Marquis, M., Averyt, K.B., Tignor, M., Miller, H.L., (Eds.), Contribution of Working Group I to the Fourth Assessment Report of the Intergovernmental Panel on Climate Change. Cambridge University Press, Cambridge, United Kingdom. Available on-line at:http://www.ipcc.ch/ipccreports/ar4-wg1.htm.

Intergovernmental Panel on Climate Change (IPCC) 2013 Climate Change 2013 *The Physical Science Basis Summary for Policymakers* ed T F Stocker et al. (Switzerland: IPCC, 2013).

Iwamura T, Possingham H P, Chades I, Minton C, Murray N J, Rogers D I, Treml E A, Fuller R A (2013) Migratory connectivity magnifies consequences of habitat loss from sea-level rise for shorebird populations. Proceedings of the Royal Society Biological Sciences 280:20130325

Jevrejeva S, Moore J C, Grinsted A (2012) Sea level projections to AD2500 with a new generation of climate change scenarios. Global and Planetary Change 80-81**:**14-20

Kirwan M, and Temmerman S (2009) Coastal marsh response to historical and future sea-level acceleration. Quaternary Science Reviews 28:1801-1808

Kirwan M L, Guntenspergen G R, D'Alpaos A, Morris J T, Mudd S M, Temmerman S (2010) Limits on the adaptability of coastal marshes to rising sea level. Geophysical Research Letters 37:L23401

Meehl G A, Hu A, Tebaldi C, Arblaster J M, Washington W M, Teng H, Sanderson B M, Ault T, Strand W G, White J B (2012) Relative Outcomes of Climate Change Mitigation Related to Global Temperature Versus Sea-Level Rise. Nature Climate Change 2:576-580

Mitsova D, Esnard A, Li Y (2012) Using dasymetric mapping techniques to improve the spatial accuracy of sea level rise vulnerability assessments. Journal of Coastal Conservation 16:355-372

Mora C, Frazier A G, Longman R J, et al. (2013) The projected timing of climate departure from recent variability. Nature 502:183-187

Morris J T, Sundareshwar P V, Nietch C T, Kjerfve B, and Cahoon D R (2002) Responses of Coastal Wetlands to Rising Sea Level. Ecology 83:2869-2877

Moore JG (1987) Subsidence of the Hawaiian Ridge, in: Decker RW, Wright TL and Stauffer PH (Eds) *Volcanism in* Hawaiʻi United States Geological Survey Professional Paper, pp. 85-100

National Oceanic Atmospheric Administration (NOAA). 2010. Mapping Inundation Uncertainty. http://csc.noaa.gov/digitalcoast/_/pdf/ElevationMappingConfidence.pdf. Accessed 13 March 2014

National Research Council (NRC) 2012 Sea-Level Rise for the Coasts of California, and Washington: Past, Present, and Fugure. Washington, DC: The National Academies Press.

Nicholls R J (2004) Coastal flooding and wetland loss in the 21st century: changes under the SRES climate and socio-economic scenarios. Global Environmental Change 14**:**69-86

Poulter B, Haplin P N (2008) Raster modeling of coastal flooding from sea-level rise. International Journal of Geographical Information Science 22**:**167-182

Rahmstorf S, Perrette M, Vermeer M (2011) Testing the robustness of semi-empirical sea level projections. Climate Dynamics 39:861-875

Reynolds M H, Berkowits P, Coutrot K N, Krause C M eds. (2012) Predicting sea-level rise vulnerability of terrestrial habit and wildlife of the Northwestern Hawaiian

Islands: U.S. Geological Survey Open-File Report 2012-1182, 139p. Available on-line at: http://pubs.usgs.gov /of/2012/1182/

Richardson M S, Gatti R C (1999) Prioritizing wetland restoration activity within a Wisconsin watershed using GIS modeling. Journal of Soil and Water Conservation 54:537-542

Rignot E, Velicogna I, van den Broeke M R, Monoghan A, Lenaerts J T M (2011) Acceleration of the contribution of the Greenland and Antarctic ice sheets to sea level rise. Geophysical Research Letters: 38

Romine B M, Fletcher C H, Barbee M M, Anderson T R, Frazier L N (2013) Are beach erosion rates and sea-level rise related in Hawaii? Global Planetary Change 108:149-157

Rotzoll K, El-Kaldi A I, Gingerich S B (2008) Analysis of an Unconfined Aquifer Subject to Asynchronous Dual-Tide Propagation 46:239-250

Rotzoll K, Fletcher C H (2012) Assessment of groundwater inundation as consequences of sea level rise. Nature Climate Change 3:477-481

Semlitsch R D, Bodie J R (1998) Are Small, Isolated Wetlands Expendable? Conservation Biology 12:1129-1133

Sallenger A H, Doran K S, Howd P A (2012) Hotspot of accelerated sea-level rise on the Atlantic coast of North America Nature Climate Change 2:884-888

Schaeffer M, Hare W, Rahmstorf S, Vermeer M (2012) Long-term sea-level rise implied by 1.5^{o}C and 2^{o}C warming levels. Nature Climate Change2:867-870

Selkoe K A, Halpern B S, Toonen R J (2008) Evaluating anthropogenic threats to Northwestern Hawaiian Islands. Aquatic Conservation: Marine and Freshwater Ecosystems 18:1149-1165

Slangen A B A, Katsman C A, van de Wal R S W, Vermeersen L L A, Riva R E M (2012) Towards regional projections of the twenty-first century sea-level change based on IPCC SRES scenarios. Climate Dynamics 38:1191-1201

Spada G, Bamber J L, Hurkmans R T W L (2013) The gravitationally consistent sea-level fingerprint of future terrestrial ice lost. Geophysical Research Letters 40:482-486

Tebaldi C, Strauss BH, Zervas CE (2012) Modelling sea level rise impacts on storm surges along US coasts Environmental Research Letters 7 014032 doi:10.1088/1748-9326/7/1/014032

U.S. Fish and Wildlife Service (2011a) James Campbell National Wildlife Refuge Comprehensive Conservation Plan and Environmental Assessment. U.S. Fish and Wildlife Service, Haleiwa, Hawaii. Available from http://www.fws.gov/uploadedFiles/Region_1/NWRS/Zone_1/Oahu_Complex/James_Campbell/Documents/James%20Campbell%20NWR%20CCP%20%28final%29%2012-01-11.pdf (accessed March 2014)

U.S. Fish and Wildlife Service, (2011b) Kealia Pond National Wildlife Refuge Comprehensive Conservation Plan and Envrionmental Assessment. U.S. Fish and Wildlife Service, Kihei, Hawaii.

U.S. Fish and Wildlife Service, (2011c) Recovery Plan For Hawaiian Waterbird Second Revision. Available on-line at: http://www.fws.gov/pacificislands/CH_Rules/Hawaiian%20Waterbirds%20RP%202 nd% 20Revision.pdf

Van Lonkhuyzen R A, Lagory K E, Kuiper J A (2004) Modeling the suitability of potential wetland mitigation sites with a geographic information system. Environmental Management 33:368-375

Vermeer M, Rahmstorf, S, (2009) Global sea level linked to global temperature. Proceedings of the National Academy of Sciences USA. 106. DOI:10.1073/pnas.0907765106

Vermeer M, Rahmstorf S, Kemp A, Horton B (2012) On the differences between two semi-empirical sea-level models for the last two millennia. Climate of the Past Discussions. 8**:**3551-3581

Vitousek S, Barbee M M, Fletcher C H, Richmond B M, Genz A S (2009) Puʻukoholā Heiau National Historic Site and Kaloko HonokōhauHistorical Park, Big Island of Hawaiʻi. Available on-line at: http://www.soest.hawaii.edu/coasts/nps/nps_report.pdf

Webb E L, Friess D A, Krauss, K W, Cahoon, D R and Guntenspergen G R (2013) A global standard for monitoring coastal wetland vulnerability to accelerated sea-level rise. Nature Climate Change 3:458-465

Wetzel F T, Kissling W D, Beissmann H, Penn D J (2012) Future climate change driven sea-level rise: secondary consequences from human displacement for island biodiversity. Global Change Biology 18:2707-2719

White D, Fennessy S (2005) Modeling the suitability of wetland restoration potential at the watershed scale. Ecological Engineering 24:359-377

Zhang, K (2011) Analysis of non-linear inundation from sea-level rise using LiDAR data: a case study for South Florida. Climatic Change 106:537-565

Zhang K, Dittmar J, Ross M, Bergh C (2011) Assessment of sea level rise impacts on human population and real property in the Florida Keys. Climatic Change 107**:**129-146